MARMARA UNIVERSITY
FACULTY OF ENGINEERING

MECHANICAL ENGINEERING DEPARTMENT

DESIGNING, ANALYZING, MANUFACTURING, AND TESTING CABLE, YARN, AND ROPE GRIPPER

Barış TAPAN, Mohamed Tharwat ELNAGAR

GRADUATION PROJECT REPORT
Department of Mechanical Engineering

Supervisor
Prof. Dr. Paşa YAYLA

ISTANBUL, 2025

MARMARA UNIVERSITY
FACULTY OF ENGINEERING

DESIGNING, ANALYZING, MANUFACTURING AND TESTING CORN YARN GRIP APPARATUS

by

Barış TAAPAN, Mohamed Tharwat ELNAGAR

July 23, 2025, Istanbul

SUBMITTED TO THE DEPARTMENT OF MECHANICAL ENGINEERING IN PARTIAL FULFILLMENT OF THE REQUIREMENTS FOR THE DEGREE

OF

BACHELOR OF SCIENCE

AT

MARMARA UNIVERSITY

Signature of Author(s) ....
Department of Mechanical Engineering

Certified By ....
Project Supervisor, Department of Mechanical Engineering

Accepted By ....
Head of the Department of Mechanical Engineering

ACKNOWLEDGEMENT

First of all, we would like to express our sincere gratitude to our supervisor, Prof. Dr. Paşa YAYLA, for his valuable guidance, continuous support, and insightful advice throughout the duration of this project. His expertise and encouragement were instrumental in the successful execution of our study.

We also extend our appreciation to Marmara University, Department of Mechanical Engineering, and the Mechanical Testing Laboratory for providing the necessary academic infrastructure and resources to carry out this research.

We would like to thank Silbak Otomotiv Sanayi ve Tic. A.Ş., a wiper manufacturing company, for granting access to their tooling workshop and CNC machinery. Their generous support enabled the manufacturing phase of our project and significantly contributed to minimizing production costs.

Furthermore, we are grateful to Darhan Yapı ve End. San. Tic. A.Ş. for supplying the steel cable samples used during our experimental tests. These samples played a crucial role in validating the performance of our design.

Finally, we acknowledge the collaborative effort and dedication of both project members throughout the research and development process.

July, 2025

Barış TAPAN
Mohamed Tharwat ELNAGAR

TABLE OF CONTENTS

ACKNOWLEDGEMENT .... *ii*
TABLE OF CONTENTS .... *iii*
ÖZET........ *vii*
ABSTRACT .... *viii*
SYMBOLS........ *ix*
ABBREVIATIONS .... *x*
LIST OF FIGURES........ *xii*
LIST OF TABLES........ *xv*

1. INTRODUCTION 1
1.1. Background........ 1
1.2. Problem Statement........ 1
1.3. Objectives and Goals of the Study 2
1.3.1 Design and Development........ 2
1.3.2 Analytical Evaluation 2
1.3.3 Finite Element Analysis (FEA)........ 3
1.3.4 Prototyping and Manufacturing........ 3
1.3.5 Experimental Validation 3
1.3.6 Knowledge Contribution 3
1.4. Literature Review 3
1.4.1 Gripping Mechanism in Tensile Testing........ 4
1.4.2 Capstan Grip Systems........ 4
1.4.3 Wedge Grips vs. Capstan Grips........ 5
1.4.4 Gap in the Literature........ 5
1.5. Review of Tensile Testing........ 6
1.5.1 Introduction 6

1.5.2 Principles of Tensile Testing 6
1.5.3 Importance of the Gripping Mechanism 6
1.5.4 Stress Concentration and Its Effects 7
1.5.5 Relevance to This Study 7
1.6. Scope of Research 7
2. DESIGN AND MANUFACTURING 9
2.1. Design Process Overview 9
2.2. Design Objectives and Constraints 9
2.3. CAD Modeling and Design Evolution 10
2.3.1 First Design – Initial Concept 10
2.3.2 Second Design – Structural Limitation Phase 11
2.3.3 Third Design – Optimized and Manufacturable Final Version 11
2.4. Material Selection 13
2.5. Manufacturing Process 14
2.5.1 Raw Material Preparation 14
2.5.2 Machining Operations 14
2.6. Assembly and Machine Fitment 16
3. STRUCTURAL SAFETY ANALYSIS AND CRITICAL POINT VALIDATION 18
3.1. Purpose of Structural Analysis 18
3.2. Governing Equations and Theoretical Background 18
3.2.1 Shear Strength of Bolts 18
3.2.2 Thread Stripping Strength 18
3.2.3 Eccentric Load Distribution 19
3.3. First Case – Eccentrically Loaded Bolted Joint 19
3.3.1 Problem Setup 19
3.3.2 Calculation 19

3.3.3 Interpretation 20
3.4. Second Case – Shaft to Plate Bolted Assembly 20
3.4.1 Problem Setup 20
3.4.2 Failure Mode Calculations 21
3.4.3 Failure Mode Comparison and Interpretation 21
3.5. Finite Element Simulation 22
3.5.1 Simulation Setup and Boundary Conditions 22
3.5.2 Load Cases and Equivalent Stress Results 23
3.5.3 Comparison with Analytical Calculations 25
4. COST ANALYSIS MATERIAL 26
4.1. Material Costs 26
4.1.1 Manufacturing Costs 26
4.2. Time Expenditure 27
4.2.1 Summary of Project Costs 27
4.3. Remarks 28
5. TEST SETUP AND PROCEDURE 29
5.1. Test Equipment 29
5.2. Significance of Material Diversity 29
5.3. Specimen Details 30
5.3.1 Material Specifications 31
5.4. Mounting Procedure 32
5.5. Test Execution 32
5.6. Post-Test Steps 33
6. RESULTS OF TENSILE TESTING 34
6.1. Test 1 – 5 mm Twisted Hemp Rope (Capstan Grip Only) 34
6.1.1 Interpretation 35
6.2. Test 2 – 6 mm Hemp Rope (Capstan vs Wedge Grip) 35

6.2.1 Interpretation 37
6.3. Test 3 – 5 mm Electrical Cable (Capstan vs Wedge Grip) 37
6.3.1 Interpretation 39
6.4. Test 4 – 2 mm Steel Wire (Capstan vs Wedge Grip) 39
6.4.1 Interpretation 42
6.5. Test 5 – 3 mm Steel Wire (Capstan vs Wedge Grip) 42
6.5.1 Interpretation 42
6.6. Test 6 – 2.5 mm Polypropylene Rope (Capstan vs Wedge Grip) 43
6.6.1 Interpretation 44
6.7. Test 7 – 1.5 mm Polypropylene Rope (Capstan vs Wedge Grip) 44
6.7.1 Interpretation 46
6.8. Summary Table of Force vs Stroke Performance 46
7. SAFETY MEASURES AND LIMITATIONS 48
7.1. Manufacturing Safety Measures 48
7.2. Laboratory Safety Measures 48
7.3. Limitaitons 48
8. CONCLUSION AND SUGGESTIONS FOR FUTURE STUDIES 511
8.1. Conclusions 51
8.2. Suggestions for Future Works 48

REFERENCES 54
APPENDICES 56
CURRICULUM VITAE 108

ÖZET

Bu proje, halat benzeri malzemelerin çekme testlerinde kullanılmak üzere tasarlanan, geliştirilen ve değerlendirilen bir Kapstan Tabanlı İplik Tutucu Düzeneği üzerine odaklanmaktadır. Temel amaç, eksenel yükleme altındaki çeşitli esnek silindirik numunelerin mekanik davranışlarını ve hasar karakteristiklerini analiz etmektir. Çalışmada, düzeneğin performansını ve yapısal sınırlarını değerlendirmek amacıyla hem sayısal hem de deneysel yöntemler kullanılmıştır.

Kenevir halat, iki farklı türde polipropilen halat, elektrik kabloları ve çeşitli çaplarda çelik tel halatlar olmak üzere birçok malzeme test edilmiştir. Kritik hasar modlarını (cıvata kesilmesi ve diş sıyırması gibi) incelemek ve izin verilebilir maksimum yükleme koşullarını belirlemek amacıyla Sonlu Elemanlar Yöntemi (FEM) analizleri ve elle hesaplamalar gerçekleştirilmiştir. Tutucunun performansı, numune üzerinde kaymayı önleme ve yükü düzgün dağıtma açısından geleneksel kama tipi tutucu ile karşılaştırılmıştır.

Deneysel sonuçlar, analitik öngörülerle yüksek düzeyde uyum göstermiş ve tutucunun yüksek yükleme altındaki testlerde numune bütünlüğünü koruma konusundaki etkinliğini doğrulamıştır. Bu öncü çalışma, özellikle esnek malzemelerle yapılan mekanik testlerde kullanılmak üzere daha güvenilir tutucu sistemlerinin tasarımına katkı sağlamaktadır. Geliştirilen sistem, malzeme mühendisliği ve mekanik test laboratuvarlarında kullanılacak test düzeneği tasarımları ve deneysel metodolojiler için sağlam bir temel sunmaktadır.

ABSTRACT

This project focuses on the design, development, and evaluation of a Capstan-based Cord Yarn Grip Apparatus intended for tensile testing of rope-like materials. The primary objective is to analyze the mechanical behavior and failure characteristics of various flexible cylindrical specimens under axial loading. The study involves both numerical and experimental approaches to assess the performance and structural limits of the apparatus.

Several materials were tested, including hemp rope, polypropylene rope (two different types), electrical cables, and steel wire ropes with varying diameters. Finite Element Method (FEM) analysis and hand calculations were performed to examine critical failure modes, such as bolt shear and thread stripping, and to determine the maximum allowable loading conditions. The grip's performance was compared with a conventional wedge grip to evaluate its efficiency in preventing slippage and distributing load uniformly across the specimen.

The experimental results showed strong alignment with the analytical predictions, confirming the grip's effectiveness in maintaining specimen integrity during high-load testing. This foundational study contributes to the design of more reliable gripping mechanisms for mechanical testing, particularly in applications involving flexible materials. The developed system provides a solid basis for future improvements in test fixture designs and experimental methodologies used in materials engineering and mechanical testing laboratories.

SYMBOLS

σ_y	Yield strength (MPa)
τ_{shear}	Shear stress (MPa)
F	Applied tensile force (N)
F_{shear}	Shear force capacity (N)
F_{strip}	Thread stripping force capacity (N)
A_s	Tensile stress area of bolt (mm^2)
d_p	Pitch diameter of thread (mm)
L_e	Thread engagement length (mm)
π	Pi (≈ 3.1416)
M	Applied moment due to eccentric loading (N·mm)
mm	millimeters
cm	centimeter
m	meter
e	Eccentricity distance (mm)
n	Number of bolts
Pa	Pascal
N	Newton
MPa	Mega Pascal
r_i	Distance of i-th bolt from centroid (mm)
$\sum r_i^2$	Sum of squared distances from centroid (mm^2)
τ_{allow}	Allowable shear stress (MPa)
τ_{strip}	Allowable thread shear stress (MPa)
F_i	Load on i-th bolt under eccentric force (N)
δ	Deformation (mm)
σ_{vm}	von Mises equivalent stress (MPa)

ABBREVIATIONS

3D – Three-Dimensional

AGS-X – Autograph Graphical Series X

ANSYS – Analysis System Software (by ANSYS Inc.)

ASTM – American Society for Testing and Materials

CAD – Computer-Aided Design

CFRP – Carbon Fiber Reinforced Polymer

CNC – Computer Numerical Control

FEA – Finite Element Analysis

FEM – Finite Element Method

FoS – Factor of Safety

ISO – International Organization for Standardization

mm – Millimeter

MPa – Megapascal

N – Newton

PP – Polypropylene

SS – Stainless Steel

UTM – Universal Testing Machine

LIST OF FIGURES

Figure 2.1 - Initial Concept – First SOLIDWORKS model 10
Figure 2.2 - Second Design – Thin Arm Profile with Risk of Bending 11
Figure 2.3 - Final Design Model 12
Figure 2.4 - Exploded View of Final Design Model 13
Figure 2.5 - 304 Stainless Steel Block and Rod 14
Figure 2.6 - CNC Milling Operation on Main Body 15
Figure 2.7 - Finished Components 16
Figure 2.8 - Capstan Grip Mounted with Steel Write and Ready to Test 17
Figure 3.1 - Ansys – Triangle Fine Mesh Generation of Bolt 23
Figure 3.2- Von Mises Stress at 13.8kN 24
Figure 3.3 - Von Mises Stress at 27.6kN 25
Figure 6.1 - Force over Stroke Curve of 5mm Hemp Rope 34
Figure 6.2 - 5mm Hemp Rope End of The Test 35
Figure 6.3 - Force over Stroke Curves of 6mm Hemp Ropes 36
Figure 6.4 - 6mm Hemp Rope Capstan Grip 36
Figure 6.5 - 6mm Hemp Rope Wedge Grip 37
Figure 6.6 - Force over Stroke Curves of 5mm Electrical Cable 38
Figure 6.7 - Electrical Cable after Testing with Capstan Grip 38
Figure 6.8 - Electrical Cable Cut Open After Test 39
Figure 6.9 - Force over Stroke Curves of 2mm Steel Wire 40
Figure 6.10 – 2mm Steel Wire after Testing with Capstan Grip 40
Figure 6.11 – 2mm Steel Wire Capstan Grip Fail Location Close-up 41
Figure 6.12- 2mm Steel Wire After Testing with Wedge Grip 41
Figure 6.13 - Force over Stroke Curves of 3mm Steel Wire 42
Figure 6.14 - Force over Stroke Curves of 2.5mm Polypropylene 43
Figure 6.15 - 2.5mm PP After Testing with Capstan Grip 44
Figure 6.16 - Force over Stroke Curves of 1.5mm Polypropylene 45

Figure 6.17 - 1.5 PP After Testing with Capstan Grip 45
Figure 6.18 - 1.5 PP After Testing with Wedge Grip 46

Figure A 1 - First Design - SolidWorks Front View 56
Figure A 2 - First Design - SolidWorks Isometric View 57
Figure A 3 - First Design - SolidWorks Right View 57
Figure A 4 - First Design - SolidWorks Back View 58
Figure A 5 - First Design - SolidWorks Isometric View from Left 58
Figure A 6 - Second Design – SolidWorks Isometric View 59
Figure A 7 - Second Design – SolidWorks Front View 59
Figure A 8 - Second Design – SolidWorks Right View 60
Figure A 9 - Second Design – SolidWorks Back View 60
Figure A 10 - Final Design - SolidWorks Isometric View 61
Figure A 11 - Final Design – SolidWorks Front View 61
Figure A 12 - Final Design – SolidWorks Left View 62
Figure A 13 - Final Design – SolidWorks Back View 62
Figure A 14 - Final Design – SolidWorks Right View 63
Figure A 15 - Final Design – SolidWorks Top View 63
Figure A 16 - Final Design – SolidWorks Clamp Jaw Close Up View 64
Figure A 17 - DARHAN - Steel Wire Test Environment 69
Figure A 18 - Example Alen Bolt 70
Figure A 19 - 1.5mm PP - Wedge Grip Test Result - 2 71
Figure A 20 - 1.5mm PP - Wedge Grip Test Result 72
Figure A 21 - 1.5mm PP – Wedge Grip Test Result Close Up 73
Figure A 22 - 1.5mm PP – Capstan Test Result 74
Figure A 23 - 1.5mm PP – Capstan Test Result Close Up 75
Figure A 24 - 2mm Steel Wire – Wedge Grip Test Result 76
Figure A 25 - 6mm Hemp Rope – Wedge grip test close up 77
Figure A 26 - 6mm Hemp Rope – Wedge Grip Test 78
Figure A 27 - 2mm Steel Wire – Before the Capstan Test 79

Figure A 28 - 2mm Steel Wire – Capstan Test Result Wide Angle 80
Figure A 29 - 2mm Steel Wire -Capstan Test Result Close up bottom................................ 81
Figure A 30 - 2mm Steel Wire – Capstan Test Result Close up upper 82
Figure A 31 - 2mm Steel Wire – Capstan Test Result 83
Figure A 32 - 5mm Electrical Cable – Copper wires after the test 84
Figure A 33 - 5mm Electrical Cable – After The Test 85
Figure A 34 - 5mm Electrical Cable – Test Result Side View 86
Figure A 35 - 5mm Electrical Cable – Test Result 87
Figure A 36 - 2.5mm PP – Test Result.. 88
Figure A 37 - 2.5mm PP – Capstan Test Result Close up 89
Figure A 38 - 2.5mm PP – Capstan Test Result.. 90
Figure A 39 - 2.5mm PP – Capstan Failure Zone Close Up 91
Figure A 40 - 6mm Hemp Rope – Test Result Close up 92
Figure A 41 - 5mm Hemp Rope - Test Result.. 93
Figure A 42 - 6mm Hemp Rope – Test Result Close up 94
Figure A 43 - 5mm Hemp Rope – Before Test 95
Figure A 44 - ANSYS - MESH Preview of Whole Body 96
Figure A 45 - ANSYS - MESH Preview of Bolts... 96
Figure A 46 - ANSYS - MESH Preview of Bolts - Iso View 97
Figure A 47 - ANSYS - Simplified Model for Simulation – Front View 98
Figure A 48 - ANSYS - 7.1kN von-Mises stress 98
Figure A 49 - ANSYS - 14kN von-Mises stress 99
Figure A 50 - ANSYS - 7.1kN CAPSTAN HOLE CLOSEUP - von-Mises stress............ 100
Figure A 51 - ANSYS – 14kN CAPSTAN HOLE CLOSEUP - von-Mises stress 100
Figure A 52 - ANSYS - 7.1kN Body Hole Close Up - von-Mises stress 101
Figure A 53 - ANSYS - 14Kn Body Hole Close Up - von-Mises stress 102
Figure A 54 - ANSYS - FoS of Bolt 13kN 102
Figure A 55 - ANSYS - FoS of Bolt - 27kN... 103
Figure A 56 - ANSYS - FOS of Simplified Model at 13kN 104
Figure A 57 - ANSYS - FOS of Simplified Model at 27kN 104

Figure A 58 – 7152N – von-Mises of Model 105
Figure A 59 - 1403N - von-Mises of Model 106
Figure A 60 - 13812N - von-Mises of Model 106
Figure A 61 - 27625N - von-Mises of Model 107

LIST OF TABLES

Table 3.1 - Failure Mode - Most critical Comparison Chart 21

Table 3.2 - ANSYS Results - Static Structure Result Chart 24

Table 4.1 - Timeline of Project 27

Table 4.2 - Summary of Costs 28

Table 5.1 - Test specimen specifications 30

Table 6.1 - Summary of Force vs Stroke Figures 47

Table A 1 - ISO 898-1 - Mechanical and physical properties of bolts 64

Table A 2 - ISO 898-1 - Mechanical and physical properties of bolts (Continued) 65

Table A 3 - ISO 898-1 - Minimum Ultimate Tensile Loads 66

Table A 4 - DARHAN - Steel Wire Tensile Test Results 68

1. INTRODUCTION

1.1. Background

Mechanical testing plays a crucial role in evaluating the structural performance of engineering materials. In particular, the tensile testing of flexible cylindrical specimens such as ropes, cables, yarns, and wires is essential in industries ranging from aerospace and marine to civil engineering and electrical applications. The accuracy and reliability of tensile test results are heavily influenced by the grip mechanism used in the test setup. Inappropriate gripping often leads to early failure, slippage, or uneven stress distribution conditions that compromise the validity of the data obtained.

Conventional wedge grips, while widely used, often fall short when testing non-rigid specimens due to their localized clamping action. This can result in crushing or slippage of soft or low-friction materials. To address this limitation, Capstan grip mechanisms have emerged as a suitable alternative. These systems rely on friction generated by wrapping the specimen around a curved surface, offering a more uniform stress distribution and improved holding capability. The Capstan principle is particularly effective for flexible and delicate materials, where minimizing localized stress and avoiding pre-test damage are critical.

1.2. Problem Statement

Despite the proven advantages of Capstan-based gripping systems, their application and study in academic contexts remain relatively limited, especially when compared to traditional wedge grips. Commercial solutions exist but are often expensive, proprietary, or not well-documented in terms of design rationale and mechanical behavior under load. As a result, there is a lack of accessible and experimentally validated Capstan grip systems suitable for universal testing machines, especially in educational or research laboratories.

Furthermore, there is a need to understand how such a grip performs across a range of specimen types, diameters, and materials—conditions typical of real-world testing environments. The mechanical integrity of the grip system itself also needs to be evaluated to ensure it can safely withstand applied loads without failure. This project aims to address these gaps by designing, analyzing, manufacturing, and testing a Capstan Yarn Grip Apparatus that can accommodate various flexible specimens and compare its performance against conventional wedge grips.

1.3. Objectives and Goals of the Study

The primary objective of this study is to design, develop, and validate a **Capstan-based Yarn Grip Apparatus** for the tensile testing of flexible, rope-like materials. This research aims to bridge the gap between theoretical design principles and practical application by creating a cost-effective, reliable, and academically documented gripping system suitable for universal testing machines.

The goals of the study are outlined as follows:

1.3.1 Design and Development

- To **conceptually and structurally design** a Capstan grip mechanism that minimizes stress concentration and slippage during axial tensile testing of flexible cylindrical specimens.
- To ensure the **mechanical integrity** of the apparatus through proper material selection, thread engagement length, and bolt arrangements.

1.3.2 Analytical Evaluation

- To perform **hand calculations** for critical failure modes such as bolt shear and thread stripping in order to estimate the **maximum allowable loading conditions**.
- To identify the **most critical point of the design**, allowing for efficient simulation focus in later stages.
- To compare different bolt grades (8.8 vs. 12.9) and justify design modifications based on strength and safety factor considerations.

1.3.3 Finite Element Analysis (FEA)

- To simulate the Capstan grip under expected load conditions using **ANSYS**, validating the stress distribution and deformation behavior.
- To compare analytical results with FEA outcomes, ensuring consistency and identifying any regions of stress concentration not apparent from calculations.

1.3.4 Prototyping and Manufacturing

- To **manufacture the grip system** using 304 stainless steel and standard CNC processes, ensuring structural robustness and compatibility with the testing machine.
- To optimize the design for **user-friendliness, assembly, and reusability** in an academic laboratory environment.

1.3.5 Experimental Validation

- To conduct tensile tests using various flexible specimens (e.g., hemp rope, polypropylene rope, steel wire rope, electrical cables) and evaluate the **grip's holding performance**.
- To assess slippage resistance and specimen integrity under test conditions, and to compare results against **conventional wedge grips**.

1.3.6 Knowledge Contribution

- To provide a **fully documented design-to-test cycle** of a Capstan grip system suitable for future academic, laboratory, or low-cost industrial applications.
- To offer **insights into failure modes**, material behavior under tensile load, and design best practices for grip mechanisms in mechanical testing.

1.4. Literature Review

The mechanical testing of flexible cylindrical materials such as ropes, cords, and cables has been a subject of practical importance in various engineering sectors, including civil infrastructure, marine systems, textiles, and electrical installations. One of the critical challenges in tensile testing of such materials lies in the design of an appropriate gripping mechanism that can hold the specimen securely without causing slippage or damage, especially under increasing tensile loads.

1.4.1 Gripping Mechanism in Tensile Testing

Traditional gripping systems such as wedge-type grips are designed primarily for rigid or semi-rigid materials. These systems utilize mechanical clamping with high normal forces to prevent slippage. However, when applied to flexible materials like yarns or synthetic ropes, these grips often cause localized stress concentrations at the clamping region. This leads to premature failure, slippage, or non-representative results, particularly for specimens with low surface friction or high compliance (ASTM D6775, 2021).

To address these limitations, friction-based gripping systems such as Capstan grips have gained attention. The Capstan principle, also known as the Eytelwein equation, relates the holding force to the number of wraps around a cylinder and the coefficient of friction between the specimen and the drum surface. This approach enables a more even stress distribution and reduces the required clamping force, thereby preserving the integrity of the test sample (Friedrich & Haufe, 2007).

1.4.2 Capstan Grip Systems

Capstan grips have been discussed in both industrial documentation and a limited number of academic publications. Commercially, Capstan grip systems are offered by manufacturers such as Instron (Instron, 2023), SD Atlas (SDL Atlas, 2022), and TestResources (TestResources, 2023). These grips are typically designed for high-strength textile materials and wire ropes, with some models capable of sustaining tensile loads up to 20 kN or more. While these systems are effective, they are often expensive, lack transparency in design rationale, and are not optimized for experimental modification or academic research.

A study by Hung et al. (2014) explored the effect of contact friction and wrap angle on Capstan grip performance for braided cords. Their findings supported the theoretical predictions of the Capstan equation, emphasizing that increased contact length and material friction led to significantly better holding performance. Similar work by Lee and Yang (2017) investigated slippage behavior in synthetic cords, demonstrating the importance of grip surface texture and wrapping angle.

However, most existing literature focuses on material behavior under tensile loads, rather than the design and analysis of the gripping mechanism itself. The grip is often treated as a black-box tool rather than a critical part of the experimental system (Coutellier et al., 2019).

1.4.3 Wedge Grips vs. Capstan Grips

Wedge grips are common in testing rigid or semi-rigid materials. They work by squeezing the specimen tightly, which can be problematic for soft materials that may slip or get damaged. Capstan grips, on the other hand, are better suited for flexible materials. They reduce the need for high clamping force and minimize the risk of damaging the sample. While wedge grips are widely used due to their simplicity and availability, Capstan grips offer better performance when testing cables, yarns, or ropes.

1.4.4 Gap in the Literature

There exists a noticeable gap in the literature regarding the academic development, mechanical analysis, and comparative testing of custom Capstan grip systems. Few studies attempt to design and manufacture a grip apparatus from first principles and validate its performance across a diverse set of specimen types. Furthermore, comparative testing against wedge grips—particularly in terms of load capacity, slippage resistance, and specimen deformation—remains limited.

This study contributes to the field by addressing these gaps. A custom Capstan Yarn Grip Apparatus was designed, manufactured, and evaluated through both numerical (FEA and hand calculations) and experimental means. Materials tested include hemp rope, two variants of polypropylene rope, electrical cable, and steel wire rope, offering a wide spectrum of mechanical and surface properties. Additionally, side-by-side comparisons with wedge-type grips provide new insight into performance differences under real loading conditions.

By documenting the full development process—from CAD design to CNC manufacturing, testing, and data evaluation—this project offers a comprehensive reference for future academic and industrial research involving grip systems for tensile testing of flexible materials.

1.5. Review of Tensile Testing

1.5.1 Introduction

Tensile testing is one of the most widely applied methods in materials engineering for evaluating mechanical properties such as strength, stiffness, and ductility. By pulling a specimen until it fractures, engineers can observe how it behaves under axial load and gather important information from its stress-strain response. These results help predict a material's performance in real-world applications, including safety, durability, and structural reliability.

1.5.2 Principles of Tensile Testing

During a tensile test, a specimen is fixed between two grips and elongated at a controlled rate. The force applied and the resulting deformation are recorded continuously. From this data, key properties such as ultimate tensile strength, yield strength, Young's modulus, and elongation at break can be derived. The shape and progression of the stress-strain curve also provide insight into the material's failure mode—whether it behaves in a brittle or ductile manner.

1.5.3 Importance of the Gripping Mechanism

While the testing process itself is standardized and well-understood, the quality of the results heavily depends on how the specimen is held in place. The gripping mechanism must secure the specimen without introducing artificial stress concentrations or causing slippage. This is particularly challenging for flexible and low-friction materials like yarns, ropes, and cables. Conventional wedge grips apply localized clamping force, which can crush or weaken the specimen at the grip interface, leading to premature failure or slippage.

1.5.4 Stress Concentration and Its Effects

One of the most critical concerns in tensile testing is stress concentration at the grip area. If the load is not transferred uniformly across the specimen, the region near the grip may experience higher localized stresses. This can cause failure at or near the grip rather than within the gauge length, resulting in invalid or non-representative test data. In flexible specimens, this problem is amplified by their tendency to deform or compress easily under pressure.

1.5.5 Relevance to This Study

To overcome these challenges, grip designs that minimize stress concentration and allow even load distribution are essential. Capstan grips offer a promising solution, especially for flexible and cylindrical specimens. By wrapping the specimen around a curved surface, they generate holding force through friction rather than clamping pressure, reducing damage and slippage. This study focuses on the design, simulation, and experimental validation of a custom Capstan Yarn Grip Apparatus, aiming to provide a reliable and repeatable solution for tensile testing of rope-like materials.

1.6. Scope of Research

This study focuses on the design, structural analysis, and experimental evaluation of a Capstan-based gripping mechanism specifically developed for tensile testing of flexible, cylindrical specimens. The apparatus is intended for use in laboratory environments with standard tensile testing machines.

The research includes:

- Conceptual and detailed design using SolidWorks CAD software,
- Analytical calculations for bolt loading, thread stripping, and load distribution,
- Finite Element Analysis (FEA) of the grip structure,
- CNC-based manufacturing of the prototype using industry-grade equipment,
- Tensile testing of multiple specimen types (hemp rope, polypropylene ropes, electrical cables, and steel wire ropes),

- Comparative performance assessment against a conventional wedge grip.

The scope of this study **does not** include:

- Optimization of the grip for cost, weight, or manufacturability,
- Fatigue, dynamic, or environmental testing (e.g., temperature, humidity effects),
- Universal compatibility with all testing machine types or extreme load ranges,
- Integration with automation or digital data acquisition systems.

The grip apparatus is dimensioned to accommodate specimens up to **20 mm in diameter**, and the test force range is determined based on material properties and mechanical safety factors validated through simulation and physical testing.

2. DESIGN AND MANUFACTURING

2.1. Design Process Overview

The design of the Capstan Yarn Grip Apparatus was driven by the functional requirements of tensile testing for flexible, cylindrical specimens such as ropes, cables, and yarns. The primary design goals included minimizing stress concentration, ensuring uniform load distribution, preventing slippage, and maintaining structural integrity under high tensile forces. To meet these criteria, a systematic engineering design approach was adopted—starting with conceptual sketches, followed by 3D modeling, analysis, material selection, and finally, manufacturing.

Computer-Aided Design (CAD) tools, specifically **SolidWorks**, were used to model the grip components. Multiple iterations were created to evaluate different geometries for the drum surface, bolt arrangements, and sample-wrapping angles. The wrap radius, frictional surface length, and clamping geometry were optimized to balance mechanical strength and ease of use. Attention was given to aligning the loading axis with the specimen centerline to reduce off-axis stresses during testing.

2.2. Design Objectives and Constraints

The Capstan Yarn Grip Apparatus was designed with the primary goal of ensuring reliable, uniform, and slippage-free gripping for rope-like specimens under axial tensile loading. The system had to fulfill key engineering constraints:

- Withstand high tensile loads (up to 7–12 kN)
- Avoid stress concentrations or early specimen failure
- Prevent bolt shear and thread stripping
- Be manufacturable with accessible tools and materials
- Fit securely into the tensile testing machine without misalignment

The design journey progressed through conceptual sketches, CAD modeling, structural analysis, and prototyping, followed by experimental validation.

2.3. CAD Modeling and Design Evolution

The mechanical design process was carried out in **SolidWorks**, progressing through three main iterations. Each design was informed by mechanical analysis, manufacturability considerations, and material constraints.

2.3.1 First Design – Initial Concept

The initial design featured a relatively narrow Capstan drum with a wrap angle limited to approximately **180°**, insufficient for achieving the necessary frictional grip. The specimen was held between **jaw-like clamps**, but this clamping mechanism introduced **high local stress concentrations** at the interface, increasing the risk of premature specimen failure or slippage during tensile loading.

Figure 2.1 shows the earliest conceptual design of the Capstan Yarn Grip. This model reflects the initial attempt at balancing wrap geometry and clamping surfaces. However, stress concentration concerns and limited wrap angle made this version suboptimal.

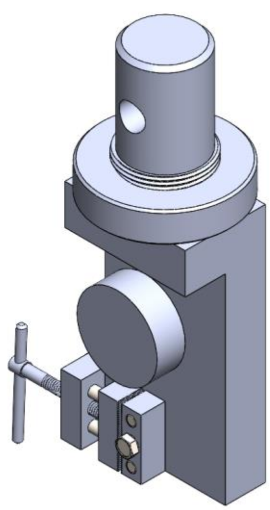

Figure 2.1 - Initial Concept – First SOLIDWORKS model

2.3.2 Second Design – Structural Limitation Phase

The second design improved upon the first by partially addressing stress distribution. The specimen clamping interface was redesigned to reduce abrupt geometry changes. However, the main body of the apparatus, especially the vertical arms supporting the Capstan drum, was **insufficient in cross-sectional thickness**. This caused the structure to behave like a cantilever under load. The **eccentric nature of the tensile force** led to expected bending stresses that exceeded safe design limits, making the design prone to **failure by elastic or plastic bending deformation** under operating loads. Additionally, **machining feasibility issues** arose due to complex surface geometry and deep internal pockets.

Figure 2.2 presents the second iteration of the design, in which the vertical arm structure was modified for better load alignment. Despite improvements, the cantilever-like behavior of the arms under eccentric loading still posed structural risks.

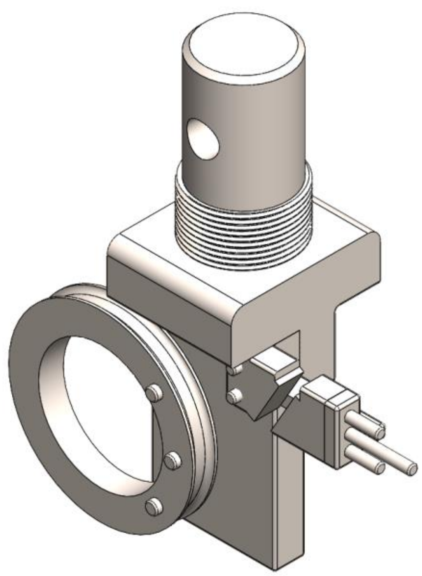

Figure 2.2 - Second Design – Thin Arm Profile with Risk of Bending

2.3.3 Third Design – Optimized and Manufacturable Final Version

The final iteration resolved both structural and manufacturability challenges. The **main body geometry was symmetrically reinforced**, allowing the tensile force to be transferred

vertically along the central axis, eliminating bending moment development. The wrap angle was increased to approximately **300°**, enhancing frictional engagement without excessive clamping force.

Modifications included:

- Thickened main body cross-section
- Widened Capstan and clamp surfaces
- Increased bolt spacing and thread depth
- Accommodation for **up to 20 mm diameter specimens**

This version also ensured compatibility with CNC milling and turning operations, allowing a balance between **mechanical robustness and ease of fabrication**.

Figure 2.3 illustrates the final optimized version of the Capstan Grip Apparatus. The structural geometry was reinforced to minimize bending, and the wrap angle was extended to improve frictional engagement.

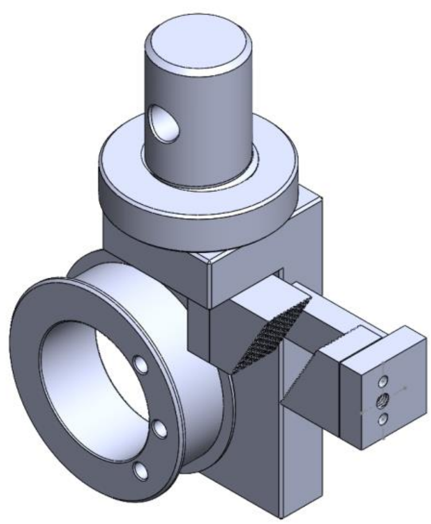

Figure 2.3 - Final Design Model

Figure 2.4 provides an exploded view of the final assembly, displaying all individual components. This helps visualize the assembly logic and highlights the modular structure of the grip.

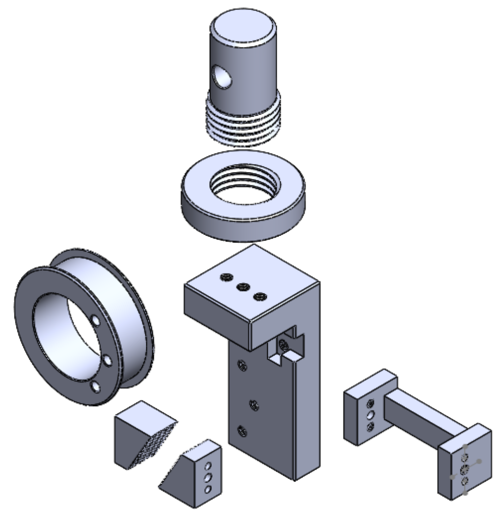

Figure 2.4 - Exploded View of Final Design Model

2.4. Material Selection

During material selection, two primary candidates were considered:

- **7000 Series High-Strength Aluminum Alloys**

  – Recommended by the project advisor for their favorable strength-to-weight ratio and ease of machining.

- **High-Strength Stainless Steel (SS)**

  – Known for superior tensile and corrosion resistance.

Although aluminum offered easier machinability, the final design imposed high contact and structural stresses. Given this, stainless steel was selected for its higher **yield strength**, **thread durability**, and **long-term structural reliability** under repeated clamping cycles. Among stainless steels, **AISI 304** was chosen for its:

- Market availability
- Cost-efficiency
- Sufficient mechanical properties for static loading applications

Despite its **reduced machinability compared to aluminum**, its performance benefits justified the additional effort.

2.5. Manufacturing Process

Manufacturing of the grip components was conducted in collaboration with **SİLBAK**, a wiper system manufacturer that provided access to their industrial CNC machines and production equipment. The fabrication was executed in a professional machine shop environment.

2.5.1 Raw Material Preparation

The raw **304 stainless steel plates and bars** were first **cut to block dimensions** using **industrial-grade band saws**. This approach minimized material waste and shortened machining cycle times, ensuring maximum use of stock dimensions for each part.

Figure 2.5 depicts the raw AISI 304 stainless steel materials used during the manufacturing phase. This photo documents the starting point before CNC machining.

Figure 2.5 - 304 Stainless Steel Block and Rod

2.5.2 Machining Operations

The following equipment was utilized:

- **Lathe Machine**: For turning the Capstan drum, shaft sections, and generating circular profiles
- **CNC Milling Machine**: For creating precise slot features, mounting holes, and interface surfaces
- **Drilling Machine**: For bolt clearance holes and alignment features
- **Surface Grinder**: To ensure flatness and fine surface finish on contact regions
- **Manual Tapping and Die Tooling**: Used to form internal and external threads for M6 bolts with high accuracy

All threading was executed manually using **lathe-guided die taps**, ensuring proper engagement with minimum backlash.

Figure 2.6 shows the CNC milling process used to machine the main body of the grip apparatus. Precision operations were essential to ensure dimensional accuracy and surface flatness for component fitment.

Figure 2.6 - CNC Milling Operation on Main Body

Figure 2.7 displays almost all machined parts after final surface finishing and threading. This highlights the readiness of components prior to assembly and testing.

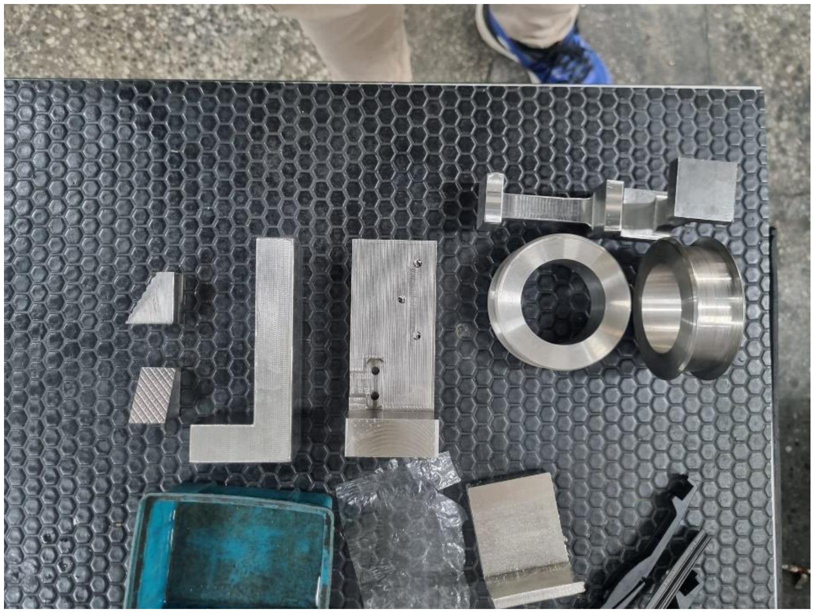

Figure 2.7 - Finished Components

2.6. Assembly and Machine Fitment

The parts were manually assembled using M6 bolts. Test fitment was performed on the Shimadzu Universal Testing Machine with alignment check. Minor adjustments were made to ensure parallelism and specimen wrap tension.

- Manual preload was applied with torque key
- Bolt threads were lubricated for uniform clamping
- Slack and misalignments were corrected before testing

Figure 2.8 illustrates the assembled Capstan Grip attached to the Shimadzu test machine with a steel wire specimen. This image provides context for how the device was integrated into the test setup.

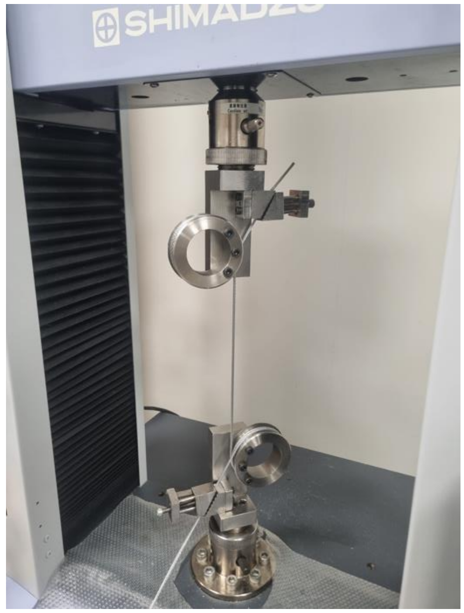

Figure 2.8 - Capstan Grip Mounted with Steel Write and Ready to Test

3. STRUCTURAL SAFETY ANALYSIS AND CRITICAL POINT VALIDATION

3.1. Purpose of Structural Analysis

The Capstan Yarn Grip Apparatus is a mechanical fixture designed to apply and withstand axial tensile forces transmitted through rope-like specimens. To ensure structural safety and eliminate the risk of premature failure, critical sections of the apparatus were analytically evaluated using engineering mechanics principles before performing Finite Element Analysis (FEA).

The purpose of these calculations is:

- To identify **the critical failure points** under peak loading conditions.
- To evaluate the **maximum safe load** that can be applied without causing bolt shear, thread stripping, or bearing failure.
- To determine **whether additional simulation (FEA)** is required for each subassembly.

3.2. Governing Equations and Theoretical Background

The two subassemblies analyzed include:

- An eccentric bolt configuration subject to vertical force (with Grade 12.9 bolts).
- A symmetric, axially loaded bolt connection between a shaft and a plate.

3.2.1 Shear Strength of Bolts

The shear strength F_{shear} is estimated from the yield strength:

$$F_{shear} = \tau_{allow} \cdot A_s \tag{1}$$

Where:

$$\tau_{allow} = 0.577 \cdot \frac{\sigma_y}{FoS} \tag{2}$$

3.2.2 Thread Stripping Strength

Thread failure occurs in the internal thread of the AISI 304 component:

$$F_{strip} = \tau_{strip} \cdot \pi \cdot d_{minor} \cdot L_e \tag{3}$$

Where:

$$\tau_{strip} = \frac{\sigma_{uts}}{2.5} \tag{4}$$

3.2.3 Eccentric Load Distribution

In case of eccentric loading, the total force is distributed non-uniformly:

$$F_i = \frac{F}{n} + \frac{M \cdot r_i}{\sum r_i^2} \tag{5}$$

Where:

- F: Total externally applied force
- n: number of bolts
- $$M = F \cdot e\ (applied\ moment\ due\ to\ eccentricity) \tag{6}$$
- r_i: Distance of the *i*-th bolt from the centroid of the bolt group
- $\sum r_i^2$: sum of the **squared distances** of all from the centroid

3.3. First Case – Eccentrically Loaded Bolted Joint

3.3.1 Problem Setup

Three M6 bolts (Grade 12.9) connect two AISI 304 stainless steel components. A vertical load is applied with a 5 mm eccentricity from the center bolt. The bolt hole layout forms a triangle.

- Bolt positions: A (0, 0), B (0, 42.43), C (8.79, 21.215) mm
- Threaded component: 20 mm thread engagement
- Material: AISI 304 (components), bolts upgraded to Grade 12.9

3.3.2 Calculation

Material Properties:

- Bolt yield strength (Grade 12.9): $\sigma_y = 1100MPa$

- Tensile stress area: $A_S = 20.1\ mm^2$
- Shear strength:

$$\tau_{allow} 0.577 \cdot 1100 = 612.7 MPa$$

$$F_{shear} = 612.7 \cdot 20.1 = 12{,}315.27N\ (per\ bolt)$$

Eccentric Load Analysis:

- Each Bolt's distance from centroid:
  - $r_A = r_B = 21.42mm, \quad r_C = 5.86mm$
  - $\sum r_i^2 = 952.5mm^2$
- Moment contribution:

$$F_{max,bolt} = \frac{F}{3} + \frac{F \cdot 5 \cdot 21.42}{952.5} = 0.4458F$$

$$0.4458F \leq 12{,}315.27 \rightarrow F \leq 27{,}625.101N$$

With Safety Factor FoS=2:

$$F_{safe} = \frac{27{,}625.101}{2} = 13{,}812.550\ N \approx 13.8\ kN$$

3.3.3 Interpretation

This analysis showed that **bolt shear** is the governing failure mode. Thread stripping was not critical due to the large engagement depth and the material properties of AISI 304. The result provided a conservative load limit for the apparatus and was used as the baseline for the FEA simulation to verify stress concentration and deformation profiles in this region.

3.4. Second Case – Shaft to Plate Bolted Assembly

3.4.1 Problem Setup

This configuration includes three M6 × 20 mm bolts connecting a shaft to a plate. The shaft is internally threaded for 12 mm; the plate is unthreaded. The applied load is purely axial and symmetric.

- Bolt material: Grade 12.9
- Threaded component: AISI 304

- Plate thickness: 12 mm

3.4.2 Failure Mode Calculations

A. Bolt Shear

- Shear strength: $60\% \cdot 1200 = 720MPa$
- Cross Section: $A = 28.27mm^2$

$$F_{shear,total} = 3 \cdot 28.27 \cdot 720 = 61{,}073N$$

B. Thread Stripping:

- Pitch Diameter: $5.35\ mm$
- Shear area per bolt: $\pi \cdot 5.35 \cdot 12 = 201.58mm^2$
- Shear strength:$0.6 \cdot 505 = 303MPa$

$$F_{strip,total} = 3 \cdot 201.58 \cdot 303 = 183{,}336N$$

C. Bearing in Plate:

- Bearing area per bolt: $6 \cdot 12 = 72mm^2$
- Bearing strength: $1.2 \cdot 505 = 606MPa$

$$F_{strip,total} = 3 \cdot 72 \cdot 606 = 130{,}896N$$

3.4.3 Failure Mode Comparison and Interpretation

Table 3.1 compares the calculated failure loads for various modes including bolt shear, thread stripping, and bearing failure. The goal is to identify the dominant failure mechanism in the shaft-to-plate assembly.

Table 3.1 *- Failure Mode - Most critical Comparison Chart*

Failure Mode	**Failure Load (N)**	**Most Critical?**
Bolt Shear	~61,073	**Yes**
Thread Stripping	~183,336	No
Bearing at Bolt Head	~130,896	No

The critical failure is bolt shear, consistent with the previous case. However, because this configuration is symmetric, lacks eccentricity, and presents no complex stress behavior, it is concluded that:

This region does not require additional Finite Element Analysis. Hand calculations are sufficient for verification.

3.5. Finite Element Simulation

To validate the hand calculation results and observe the stress distribution under realistic loading, a simplified 3D Finite Element Analysis (FEA) was conducted using **ANSYS Mechanical 2023**. The goal was to confirm the structural safety of the grip's most critical bolted region under eccentric tensile force application.

3.5.1 Simulation Setup and Boundary Conditions

A simplified geometry of the Capstan Yarn Grip was used to ensure computational efficiency. Unnecessary features were removed, and a **rectangular block was added to simulate rope contact**. The tensile force was applied vertically from the **bottom face of this block**, representing the external loading transmitted by the rope through the capstan drum.

- **Bolt Simulation**: Three simplified bolts (5.2 mm diameter) were modeled in place of M6 screws.
- **Mesh Details**:
    - Global element size: 1.0 mm
    - Mesh type: Triangular surface elements
    - Mesh refinements: Applied around bolt holes and clamping areas using *face meshing* and *local refinement*
- **Contact Definitions**:
    - Screw to body: Bonded
    - Screw to capstan: Frictional contact (default coefficient)
    - Capstan to body: Frictionless

- **Supports**: The upper surface of the main grip body was fixed to simulate attachment to the tensile testing machine.
- **Load Application**: Tensile force was applied vertically at the simulated rope contact block with an eccentricity of 5 mm from the centroid of the bolt triangle.

Figure 3.1 shows the mesh configuration used in the FEA analysis. A fine triangular mesh was applied around the bolt region to capture stress gradients accurately.

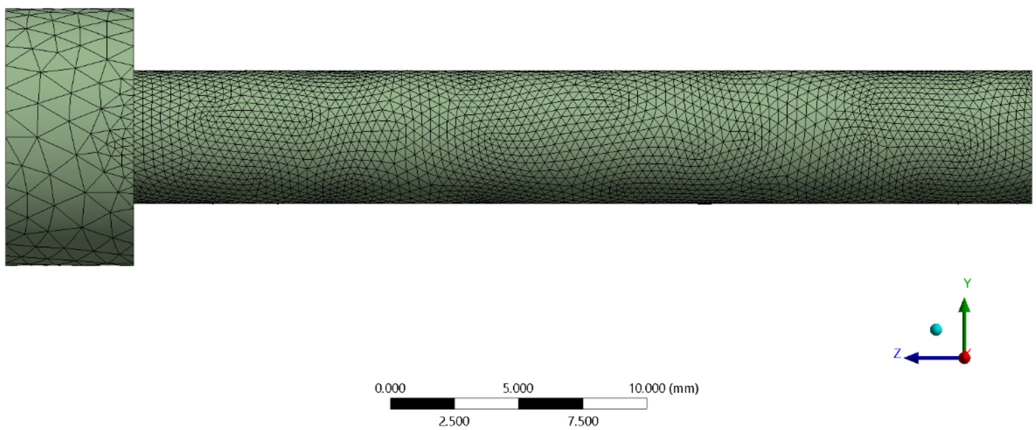

Figure 3.1 - Ansys – Triangle Fine Mesh Generation of Bolt

3.5.2 Load Cases and Equivalent Stress Results

To assess the structural response of the Capstan Grip Apparatus under eccentric loading, simulations were conducted at multiple load levels. These levels included:

- **4,000 N**: Representing low-load condition for initial verification
- **7,152 N**: Half of the analytically determined safe load
- **7,500 N**: Slightly above mid-range
- **10,000 N**: Moderate overload case
- **13,812 N**: Equivalent to the **maximum allowable load with FoS = 2**
- **27,625 N**: Equivalent to the **yield threshold (FoS = 1)**

Table 3.2 summarizes the maximum von Mises stress and deformation values from FEA simulations under different loading conditions. This data is used to validate hand-calculated stress limits and evaluate structural safety.

__Table 3.2__ - ANSYS Results - Static Structure Result Chart

Load (N)	Max von Mises Stress (MPa)	Max Deformation (mm)
4000	311.21	1.4767×10^{-3}
7500	634.41	3.0083×10^{-3}
10000	876.15	4.1543×10^{-3}
13812	1251.1	5.9324×10^{-3}
27625	2636.5	1.3222×10^{-2}

Figure 3.2 presents the von Mises stress distribution at the calculated safe design load (13.8 kN). The stress is concentrated around bolt holes.

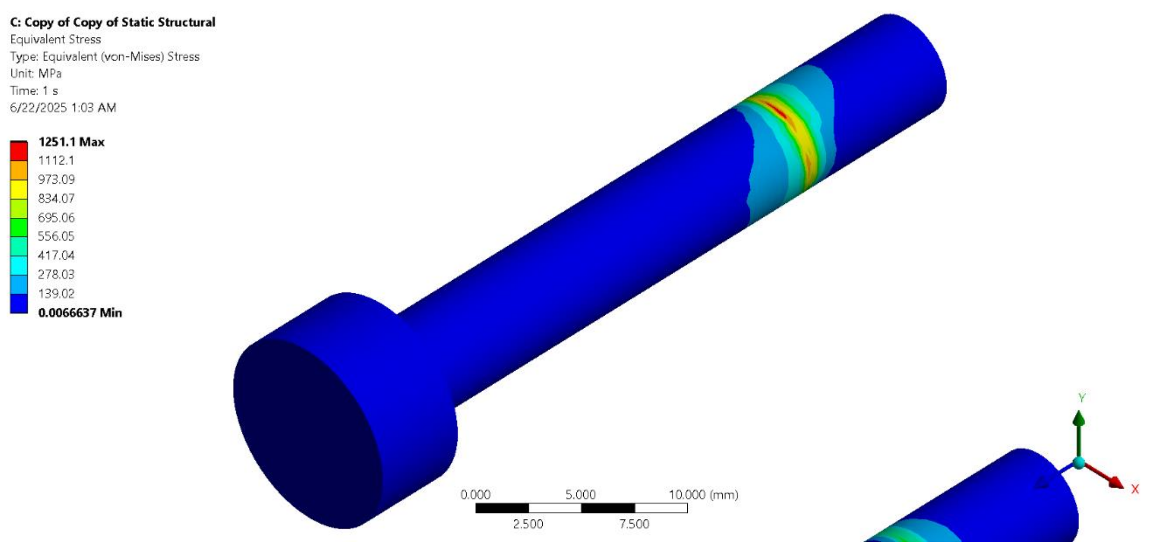

Figure 3.2- Von Mises Stress at 13.8kN

Figure 3.3 displays the von Mises stress when the load is doubled (27.6 kN), representing the failure threshold. This helps verify safety margins and identify potential failure zones.

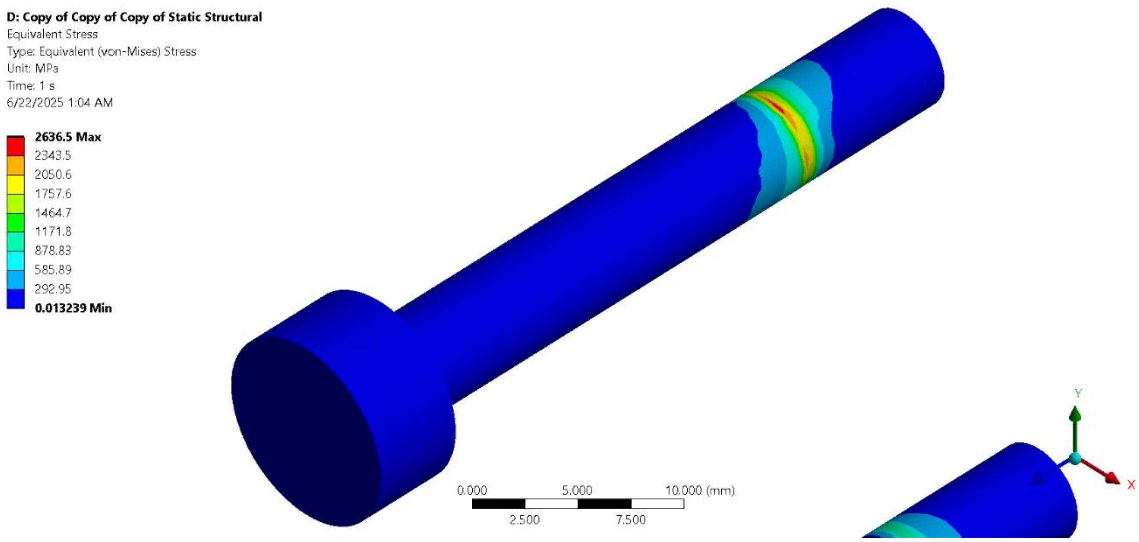

Figure 3.3 - Von Mises Stress at 27.6kN

3.5.3 Comparison with Analytical Calculations

The simulation findings are now compared to the hand-calculated results based on bolt shear stress. The theoretical shear stress on the most loaded bolt was calculated as:

$$\tau_{calc} = \frac{0.4458 \cdot 13{,}812N}{20.1} \approx 306.1Mpa$$

Where:

- 0.4458 represents the force fraction due to eccentric load
- 20.1 mm^2 is the tensile stress area of the M6 bolt

Using the empirical shear strength approximation:

$$\tau_{allow} = \frac{0.557 \cdot 1100}{2} = 317.35\ MPa$$

Which confirms that the **hand-calculated safe load of 13.8 kN** is consistent with the onset of yielding in the FEA.

In contrast, the **FEA outputs von Mises stress**, which combines axial and shear components in a multiaxial stress state. The peak von Mises stress at 13.8 kN is approximately **1,251 MPa**, slightly exceeding the 1100 MPa yield limit of Grade 12.9 bolts. This discrepancy is expected due to localized stress concentration zones around bolt holes and contacts.

4. COST ANALYSIS MATERIAL

A comprehensive evaluation of the cost and time spent on the development of the Capstan Yarn Grip Apparatus was conducted to assess the feasibility and efficiency of the project. The total expenditure includes raw material costs, manufacturing efforts, and specimen procurement, as outlined below.

4.1. Material Costs

- **AISI 304 Stainless Steel (Raw Material):** The primary structural components of the apparatus were machined from AISI 304 stainless steel blocks and rods. The raw material was purchased from a local supplier at a total cost of **approximately 2,000 TL**.
- **Steel Wire Rope Samples:** Steel wire specimens used in tensile tests were generously **provided free of charge by DARHAN**, a partner company supporting the experimental phase.
- **Other Test Samples (Hemp, Polypropylene, Electrical Cable):** These materials were sourced from various suppliers. While exact prices were not documented, the individual sample costs were minor. The total cost for all non-metallic specimens is **estimated to be less than 500 TL** in total. Given the quantity and low unit prices, their financial impact is considered **negligible**.

4.1.1 Manufacturing Costs

The fabrication process took place over the course of **three weeks**, including:

- CNC machining of the capstan drum and body components
- Manual thread tapping and finishing
- Surface preparation and minor reworks after test fittings
- Assembly trials and grip alignment on the Shimadzu UTM

Although the project was conducted within a university-supported environment with industrial partner access (SİLBAK), a realistic approximation of the **manufacturing cost is**

10,000 TL. This estimate includes machine time, labor effort, tool wear, and workshop overheads.

4.2. Time Expenditure

Table 4.1 outlines the estimated durations for each project phase from design to testing. This timeline helps reflect the planning and time investment for the development cycle.

The development timeline can be summarized as follows:

Table 4.1 *- Timeline of Project*

Phase	Estimated Duration
Design and CAD Modelling	1 week
Structural Analysis & Optimization	1 week
Manufacturing and Fitment Trials	3 weeks
Test Setup and Execution	1 week
Data Analysis and Documentation	1 week
Total Project Time	**~7 weeks**

This timeline reflects the effort invested in not only physical production but also engineering calculations, finite element simulations, and test preparations.

4.2.1 Summary of Project Costs

Table 4.2 details the cost of distribution across raw materials, manufacturing, and specimen procurement. This cost analysis is important for evaluating the economic feasibility of the design.

__Table 4.2__ - Summary of Costs

Item	Estimated Cost (TL)
Stainless Steel Raw Material	2,000 TL
Manufacturing (CNC + Manual)	10,000 TL
Purchased Samples (non-steel)	500 TL (approx.)
Steel Wire Samples (DARHAN)	0 TL (sponsored)
Total Estimated Cost	**12,500 TL**

4.3. Remarks

The total estimated project cost is approximately **12,500 TL**, which includes both tangible material expenses and realistic approximations of industrial-level manufacturing services. Time-wise, the project spanned over **seven weeks**, highlighting the iterative nature of design, optimization, and physical testing required for a custom mechanical fixture. The support of industrial partners like DARHAN and SİLBAK significantly reduced costs and accelerated development.

5. TEST SETUP AND PROCEDURE

To assess the performance of the Capstan Yarn Grip Apparatus, tensile tests were conducted using a **Shimadzu AGS-X Universal Testing Machine** located in the Mechanical Testing Laboratory at Marmara University. The aim was to evaluate the grip's ability to secure various flexible specimens without slippage or premature failure under axial loading, and to compare its effectiveness with conventional wedge grips.

5.1. Test Equipment

The tensile tests were conducted using a **Shimadzu AGS-X** Series universal testing machine with a maximum load capacity of **50 kN**. The system was operated through the **Trapezium X** testing software, which facilitated precise control and data acquisition throughout the experiments. A **high-accuracy**, calibrated load cell was employed to ensure reliable force measurements. The tests were performed at a constant crosshead displacement rate of **10 mm/min**, adhering to standardized testing protocols. All experiments were carried out under laboratory ambient conditions, maintained at approximately **23 ± 2°C**, to minimize environmental influence on material behavior.

5.2. Significance of Material Diversity

The wide range of mechanical and surface properties among the samples posed different challenges to the grip system. For example:

Hemp rope, being rough and fibrous, created high friction but was prone to uneven loading if not aligned properly.

Polypropylene ropes were more prone to slippage due to their low surface friction, making them ideal for evaluating grip effectiveness.

Electrical cables tested the grip's ability to hold multi-layered specimens without damaging outer insulation.

Steel wire ropes, due to their high tensile strength and stiffness, served as the most demanding material, testing the grip's structural integrity and clamping performance under high loads

5.3. Specimen Details

Table 5.1 lists the physical and material characteristics of the test specimens used in this study. These specifications are crucial for interpreting the tensile test results accurately.

Four types of flexible materials were tested:

Table 5.1 *- Test specimen specifications*

Name of Specimen	**Diameter (mm)**	**Length (m)**	**Weight (grams)**
Hemp Rope	≈ 5.0	≈ 1.0	20.2959
Hemp Rope	≈ 6.0	≈ 1.0	24.3551
Polypropylene Rope	≈ 1.5	≈ 1.0	1.875
Polypropylene Rope	≈ 2.5	≈ 1.0	5.199
Electrical Cable	≈ 5.0	≈ 1.5	180.059
Steel Wire	2.0	≈ 3.5	67.7235
Steel Wire	3.0	≈ 4.4	180.344

Each specimen was prepared in lengths of **1.0 m to 4.0 m**, depending on the material and test configuration. The test length was set to be **25.0 cm** (distance between Before testing, all specimens were **weighed using a precision digital scale** to document mass and ensure consistency between trials. This also enabled mass-based comparisons related to mechanical strength and material density.

5.3.1 Material Specifications

In this study, four different types of rope-like materials were tested to evaluate the performance of the Capstan Yarn Grip Apparatus. Each material has unique mechanical and surface characteristics, which helped assess the grip's ability to hold specimens with different levels of stiffness, texture, and friction. The following sections describe the general features of each tested material.

5.3.1.1. Hemp Rope

Hemp rope is a natural fiber material with a rough surface and moderate mechanical strength. It is commonly used in industrial and agricultural applications. The rope used in this study had a twisted fiber structure, which created a high-friction surface. This made it suitable for testing how well the grip could prevent slippage and handle uneven loading. The rope's rough texture and irregular shape also made it useful for studying grip behavior under non-ideal conditions.

5.3.1.2. Polypropylene Rope

Two types of polypropylene rope were included in the tests:

- **2.5mm (braided):** This rope had a tightly woven surface, which made it more flexible and smoother. During testing, it showed ductile behavior, with fibers stretching before failure.
- **1.5mm (twisted):** This rope had a loose, spiral shape. It was more prone to slipping and breaking quickly, with less elongation.

Polypropylene is a lightweight plastic material with low surface friction. These ropes helped examine how the grip performs with soft, low-friction specimens that are harder to secure.

5.3.1.3. Electrical Cable

The electrical cable consisted of a copper core with an insulating outer layer made of plastic. The cable's surface was smooth, and the internal structure had multiple layers. Because of this, it was challenging to grip without damaging the insulation. The cable showed moderate strength and elastic deformation. It was tested to check if the grip could hold layered or coated specimens without causing surface damage.

5.3.1.4. Steel Wire Rope

Steel wire rope was the strongest material tested in this study. Two diameters were used: **2 mm** and **3 mm**. These ropes were made of multiple steel wires twisted together in a helical pattern. The surface was smooth and metallic, with very low flexibility. These samples were used to test the grip under high loads and to see if it could prevent slippage with hard, stiff materials. Because of their high strength and low deformation, these ropes also helped test the grip's mechanical limits.

5.4. Mounting Procedure

The Capstan grip was securely mounted onto the Shimadzu universal testing machine using the adapters to ensure mechanical stability and proper alignment. Test specimens were wrapped around the Capstan drum at an angle of approximately 300°, thereby increasing the effective contact area and enhancing frictional resistance to slippage during loading. The free ends of each specimen were positioned within the bolted clamping mechanism, where initial manual tension was applied, followed by the application of full torque to the bolts to achieve firm fixation. Throughout the mounting process, careful attention was paid to maintaining axial alignment of the specimen to prevent eccentric loading and potential bending effects. Prior to the commencement of data acquisition, a preload of approximately 20 N was applied to eliminate slack and ensure the specimen was properly seated within the gripping system.

5.5. Test Execution

The tensile testing procedure was carried out under controlled conditions to ensure consistency and reliability of the collected data. All experiments were conducted in accordance with standardized mechanical testing protocols, with real-time monitoring and data acquisition enabled through the integrated testing software. The following steps outline the procedure employed during test execution:

- The tensile tests were conducted using automated control via the Trapezium X software platform, which continuously recorded both applied force and crosshead displacement throughout each test.
- Each specimen was subjected to uniaxial tensile loading until either material failure occurred within the gauge length or noticeable slippage was detected at the gripping interface.
- For each material group, the tests were performed in duplicate, once using a conventional wedge grip and once using the Capstan grip, to enable comparative evaluation of gripping performance.

5.6. Post-Test Steps

- The failure mode was noted (clean rupture, insulation damage, slippage, etc.).
- The grip was visually inspected for signs of wear or deformation.
- Surfaces were cleaned between tests to maintain uniform contact conditions.
- Data was exported for later analysis of stress-strain behavior and comparison across grip types.

This systematic approach ensured consistency across test conditions and enabled a robust evaluation of the grip's mechanical performance across different specimen types and dimensions.

6. RESULTS OF TENSILE TESTING

This section presents the experimental observations and mechanical behavior of various rope-like specimens subjected to uniaxial tensile loading using both Capstan and Wedge grip systems. Force versus stroke curves are analyzed to evaluate grip performance in terms of slippage resistance, stress uniformity, and failure characteristics. Tests were conducted under controlled laboratory conditions using the Shimadzu AGS-X universal testing machine. For some materials, Wedge grip tests could not be completed due to compatibility limitations or excessive slippage, which are noted in the respective subsections.

6.1. Test 1 – 5 mm Twisted Hemp Rope (Capstan Grip Only)

The Capstan grip was able to maintain full engagement throughout the tensile test of the 5 mm twisted hemp rope. The force–stroke curve exhibited a gradually increasing trend with small oscillations, indicative of micro-fiber adjustments within the twisted structure. Peak force reached just under 1000 N, with a relatively smooth failure near the end of the gauge length, suggesting uniform stress distribution.

Figure 6.1 illustrates the tensile force versus stroke behavior of the 5 mm twisted hemp rope. The gradual force rise with fiber adjustment oscillations demonstrates ductile characteristics.

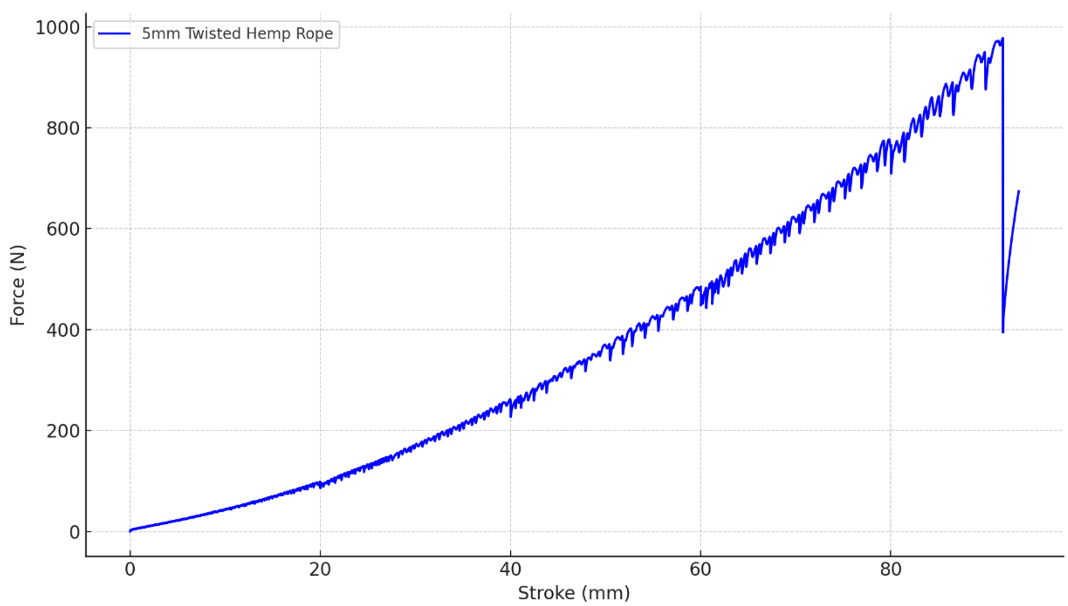

Figure 6.1 - Force over Stroke Curve of 5mm Hemp Rope

Figure 6.2 shows the visual outcome of the hemp rope after testing. The fracture location confirms failure occurred within the gauge length, validating proper grip performance.

Figure 6.2 - 5mm Hemp Rope End of The Test

6.1.1 Interpretation

The Capstan grip effectively mitigated stress concentrations at the grip interface. The observed failure pattern confirms that the rope failed in the gauge section, validating proper alignment and load transfer. The absence of early failure or slippage demonstrates the grip's suitability for twisted natural fibers.

6.2. Test 2 – 6 mm Hemp Rope (Capstan vs Wedge Grip)

The comparison of Force–Stroke responses shows a clear performance gap. The Capstan grip enabled the sample to withstand over 2400 N with a long stroke (≈35 mm), while the wedge grip failed prematurely (~1800 N at ≈90 mm), with noticeable slippage.

Figure 6.3 compares the performance of the Capstan and Wedge grips for 6 mm hemp rope. The Capstan grip sustained higher loads with more consistent behavior.

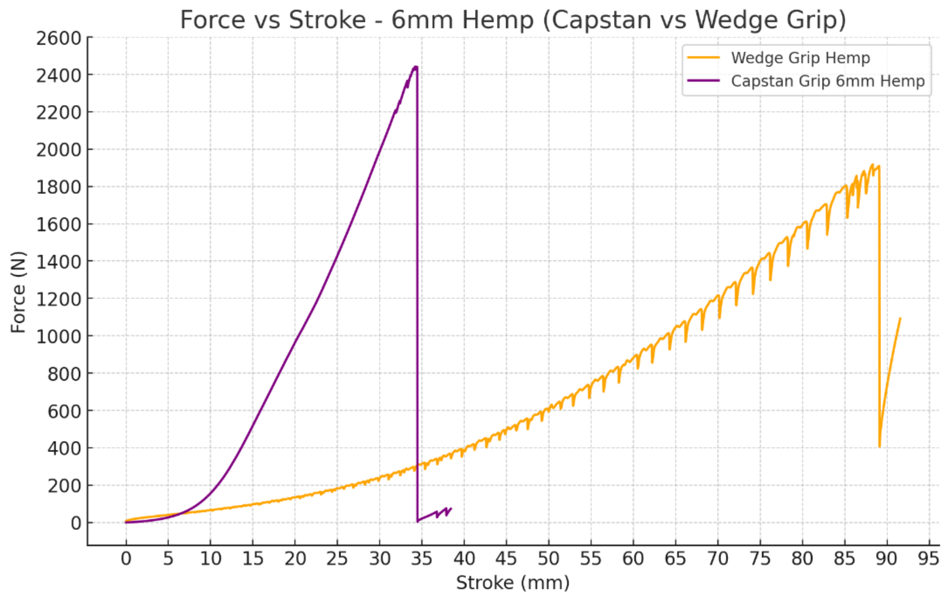

Figure 6.3 - Force over Stroke Curves of 6mm Hemp Ropes

Figure 6.4 shows the specimen after testing with the Capstan grip. The rupture appears clean and centered, indicating even stress distribution.

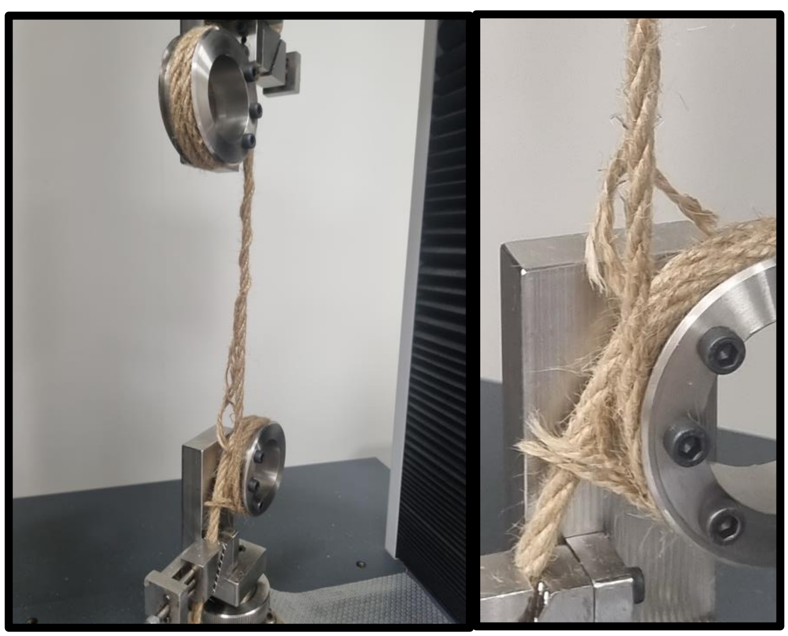

Figure 6.4 - 6mm Hemp Rope Capstan Grip

Figure 6.5 shows the failure of the 6 mm hemp rope tested with a Wedge grip. The uneven rupture and deformation indicate stress concentration and slippage at the grip interface.

Figure 6.5 - 6mm Hemp Rope Wedge Grip

6.2.1 Interpretation

The Capstan grip's distributed frictional interface allowed for higher stress capacity and reduced stress concentration, leading to a cleaner rupture. The Wedge grip induced progressive slipping, evidenced by the jagged force pattern, and compromised the accuracy of the test. This test highlights the superior adaptability of the Capstan system for rough-surfaced hemp materials.

6.3. Test 3 – 5 mm Electrical Cable (Capstan vs Wedge Grip)

The Wedge grip test showed early damage initiation, with force fluctuations around 800–1000 N, indicating insulation tearing and slippage. The Capstan grip achieved a peak force near 1200 N, with a longer stroke and more stable curve.

Figure 6.6 presents a comparison of force vs. stroke behavior for 5 mm electrical cables using Capstan and Wedge grips. The Capstan grip curve is smoother and extends longer, suggesting more controlled failure.

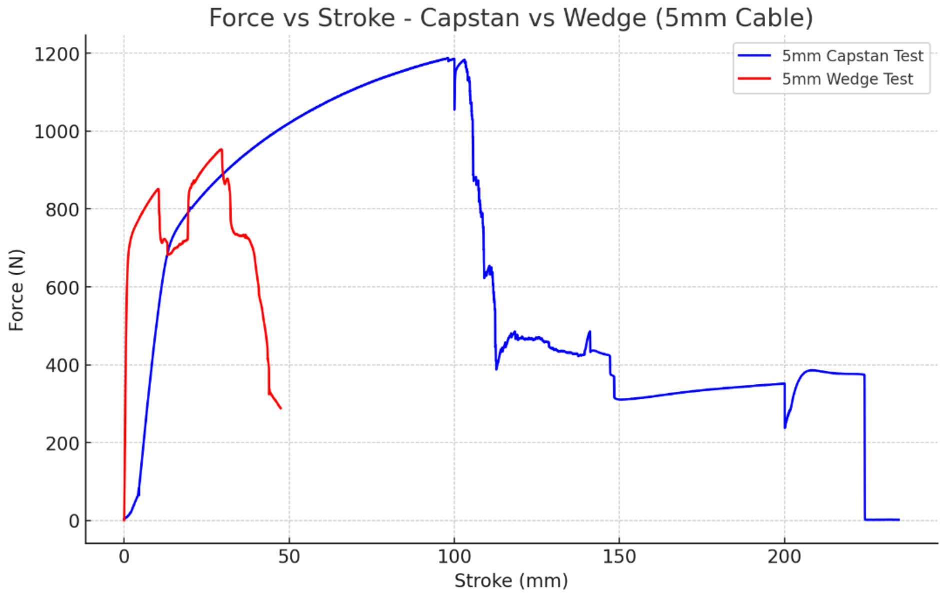

Figure 6.6 - Force over Stroke Curves of 5mm Electrical Cable

Figure 6.7 shows the cable after testing with the Capstan grip. The insulation remains mostly intact, showing the grip prevented crushing.

Figure 6.7 - Electrical Cable after Testing with Capstan Grip

Figure 6.8 reveals the internal structure of the cable post-failure. This provides evidence of intact copper strands, confirming no internal breakage during testing.

Figure 6.8 - Electrical Cable Cut Open After Test

6.3.1 Interpretation

Multi-layered cables are prone to outer sheath rupture when clamped unevenly. The Capstan grip provided a controlled load application, reducing localized compression on the insulation. This test demonstrates the effectiveness of the Capstan grip in preserving structural integrity in composite specimens.

6.4. Test 4 – 2 mm Steel Wire (Capstan vs Wedge Grip)

The Wedge grip failed at ≈3400 N with a sharp drop in force, likely due to specimen slippage or grip failure. Conversely, the Capstan grip enabled the wire to reach ≈4100 N with a smooth linear curve and clean fracture.

Figure 6.9 compares the response of 2 mm steel wire tested under both grip types. The Capstan grip achieved higher loads and cleaner failure without abrupt force drops.

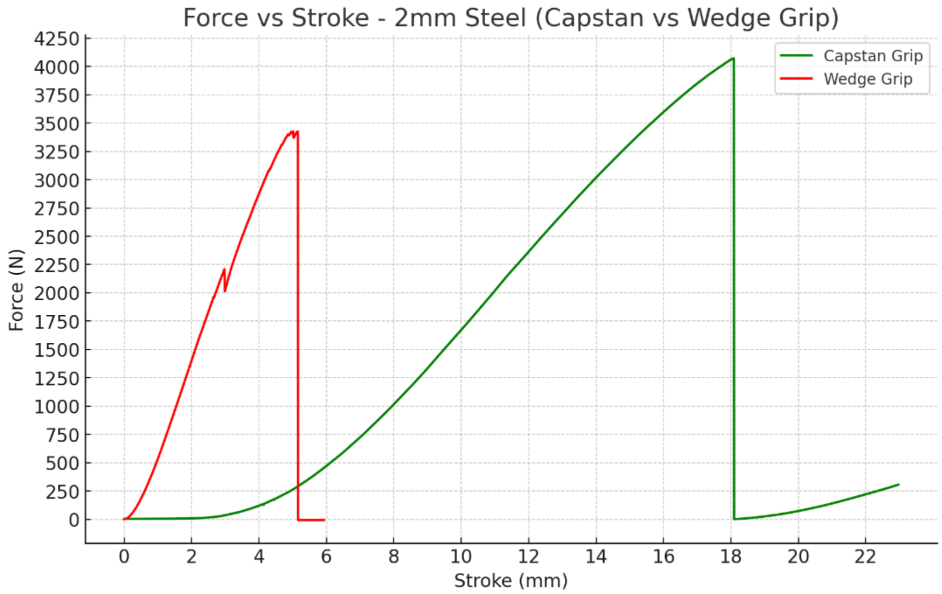

Figure 6.9 - Force over Stroke Curves of 2mm Steel Wire

Figure 6.10 displays the steel wire following failure under Capstan grip. The clean fracture at mid-span confirms effective axial loading.

Figure 6.10 – 2mm Steel Wire after Testing with Capstan Grip

Figure 6.11 is a zoomed-in view of the failure point in the Capstan grip setup, showing fracture propagation aligned with the axial load direction.

Figure 6.11 – 2mm Steel Wire Capstan Grip Fail Location Close-up

Figure 6.12 shows failure after Wedge grip testing. Early slippage and necking are visible near the grip area, indicating grip-induced stress issues.

Figure 6.12- 2mm Steel Wire After Testing with Wedge Grip

6.4.1 Interpretation

Steel wires possess high stiffness and low friction, posing a challenge for mechanical clamping. The Capstan grip succeeded in maintaining contact without slippage. This test confirms that the design can withstand high axial loads without compromising specimen behavior or causing premature failure.

6.5. Test 5 – 3 mm Steel Wire (Capstan vs Wedge Grip)

The Capstan grip achieved ≈7000 N of peak force with clear post-yield behavior, while the Wedge grip peaked at ≈6600 N with abrupt failure. The Capstan curve is longer, showing more plastic deformation.

Figure 6.13 compares the mechanical behavior of 3 mm steel wire under both grip types. The Capstan grip allowed greater ductility before rupture.

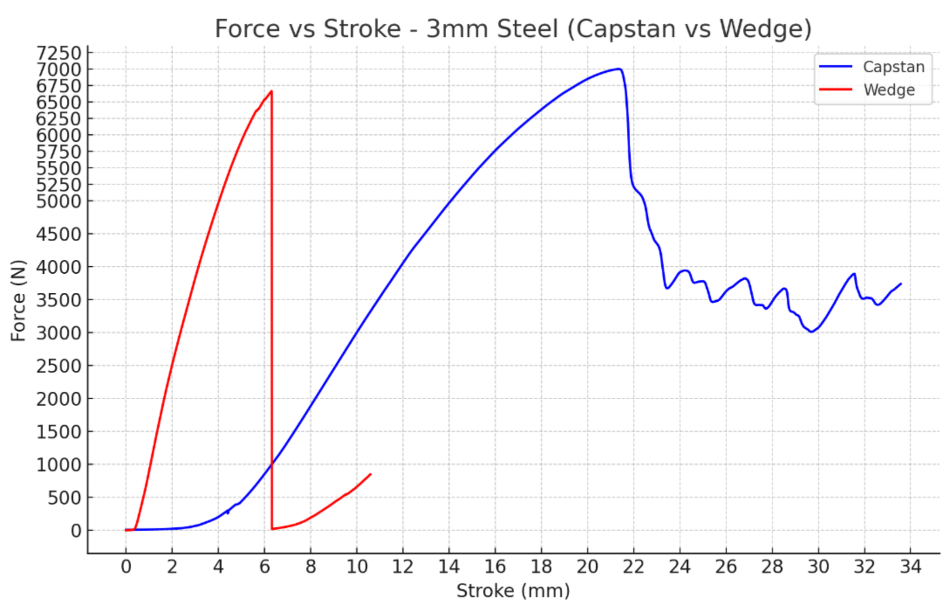

Figure 6.13 - Force over Stroke Curves of 3mm Steel Wire

6.5.1 Interpretation

The Capstan grip maintained axial alignment and load distribution even at elevated force levels, validating its structural robustness. The Wedge grip, though close in maximum force, lacked the stability to sustain deformation post-yield, demonstrating a failure likely linked to grip slippage or stress concentration.

6.6. Test 6 – 2.5 mm Polypropylene Rope (Capstan vs Wedge Grip)

The Capstan grip reached ≈1350 N with a long, gradual curve indicating ductile failure. The Wedge grip failed earlier (~800 N), and the stroke was significantly shorter, suggesting poor load transfer and premature specimen disengagement.

Figure 6.14 illustrates tensile performance for 2.5 mm polypropylene rope. Capstan grip results show higher strength and a more progressive failure mode.

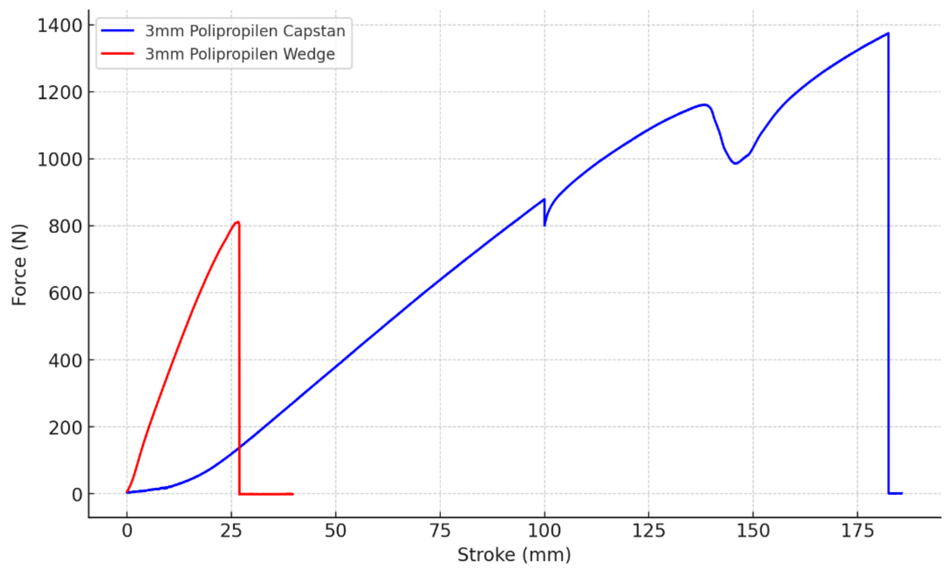

Figure 6.14 - Force over Stroke Curves of 2.5mm Polypropylene

Figure 6.15 shows the polypropylene rope specimen after tensile testing with the Capstan grip. The image highlights clean elongation and fracture, confirming successful grip performance.

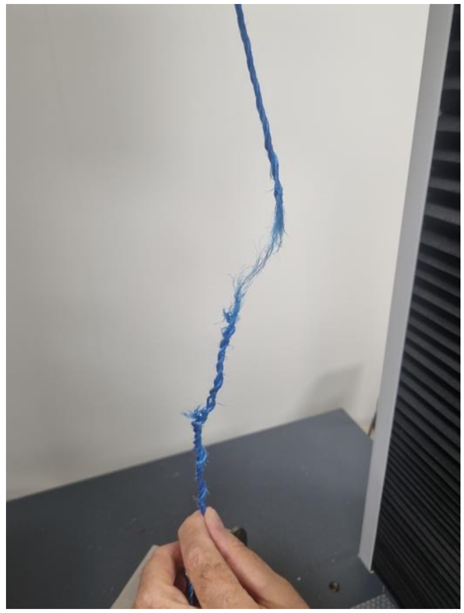

Figure 6.15 - 2.5mm PP After Testing with Capstan Grip

6.6.1 Interpretation

Due to polypropylene's low friction coefficient, Wedge grips tend to underperform. The Capstan grip utilized surface wrapping to create frictional engagement, preserving specimen integrity and enabling full-range tensile behavior.

6.7. Test 7 – 1.5 mm Polypropylene Rope (Capstan vs Wedge Grip)

The Capstan grip achieved ≈700 N at ≈85 mm stroke, indicating full ductile elongation. The Wedge grip test showed early termination around ≈450 N and signs of sudden slippage.

Figure 6.16 compares the tensile performance of 1.5 mm polypropylene rope under both grip types. The Capstan grip achieved greater elongation and force before failure.

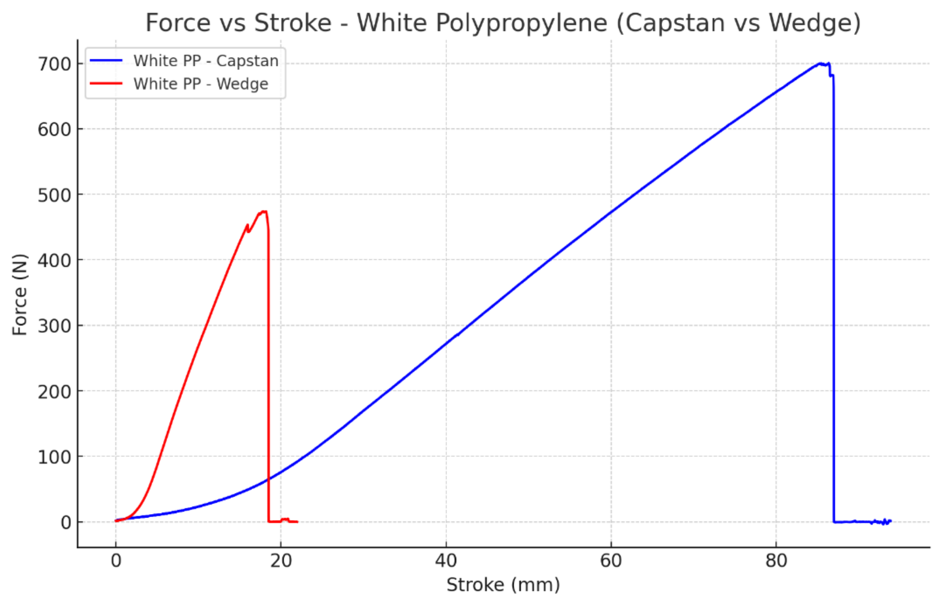

Figure 6.16 - Force over Stroke Curves of 1.5mm Polypropylene

Figure 6.17 displays the failed specimen after testing with the Capstan grip. The material deformed uniformly, suggesting well-distributed tensile loading.

Figure 6.17 - 1.5 PP After Testing with Capstan Grip

Figure 6.18 shows the same specimen tested with the Wedge grip. Failure occurred prematurely with signs of slippage and localized damage.

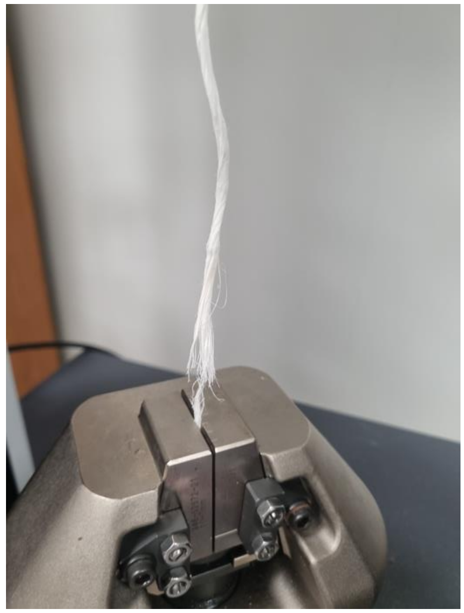

Figure 6.18 - 1.5 PP After Testing with Wedge Grip

6.7.1 Interpretation

This test underscores the inadequacy of conventional wedge systems for fine-diameter, low-friction specimens. The Capstan grip provided uniform stress application and facilitated reliable mechanical testing of small polymeric samples.

6.8. Summary Table of Force vs Stroke Performance

Table 6.1 consolidates the maximum tensile forces and failure modes observed for each specimen and grip combination. It offers a clear comparison between Capstan and Wedge grips.

Table 6.1 - Summary of Force vs Stroke Figures

Material	Max Force – Capstan (N)	Max Force – Wedge (N)	Observed Failure Mode	Comments
5 mm Hemp	~1000	–	Mid-span rupture	Smooth, stable behavior
6 mm Hemp	~2400	~1800	Capstan: rupture; Wedge: slippage	Capstan superior
5 mm Cable	~1200	~1000	Capstan: insulation necking; Wedge: erratic	Capstan preserved sample
2 mm Steel Wire	~4100	~3400	Capstan: clean break; Wedge: early fail	Grip validation test
3 mm Steel Wire	~7000	~6600	Capstan: gradual failure	High-load capacity proven
2.5 mm PP	~1350	~800	Capstan: ductile	Wedge failed prematurely
1.5 mm PP	~700	~450	Capstan: clean elongation	Capstan succeeded, wedge slipped

7. SAFETY MEASURES AND LIMITATIONS

7.1. Manufacturing Safety Measures

Although we only supervised the manufacturing and testing processes, several standard safety measures should be followed during such activities. In the laboratory, personal protective equipment (PPE) such as safety goggles and lab coats should be worn, and a safe distance maintained during tensile testing to avoid injury from sudden specimen failure. Machines must be inspected before use, and emergency stop buttons should be easily accessible. In CNC workshops, only trained personnel should operate the machines with all protective enclosures in place, and toolpaths should be verified before machining. Proper material handling and awareness of sharp or heavy components are also essential to ensure a safe working environment.

7.2. Laboratory Safety Measures

In the school laboratory, safety measures should always be followed during testing. It is important to stay clear of the tensile testing machine while it is running, as it applies high forces that may cause sudden specimen failure. No one should be near the moving parts during operation, and all observations should be made from a safe distance. The emergency stop button must always remain accessible, and the area around the machine should be kept clear to avoid accidents.

7.3. Limitations

Although the Capstan Yarn Grip Apparatus was successfully designed, manufactured, and tested under controlled laboratory conditions, several technical and methodological limitations emerged throughout the study. These limitations should be critically acknowledged, as they affect the scope, generalizability, and robustness of the conclusions drawn.

One of the primary constraints was the limited diversity of the test specimens. While a representative selection of flexible materials—such as hemp rope, polypropylene cord, electrical cable, and steel wire—was included, the range did not encompass specialized industrial materials such as aramid fibers (e.g., Kevlar), thermoplastic elastomers, or biomedical sutures. As a result, the applicability of the grip system to more advanced or application-specific materials remains unexplored.

Additionally, the geometric design of the apparatus imposed strict dimensional constraints. The system was optimized for specimens up to 20 mm in diameter; therefore, specimens significantly smaller or larger than this range could not be accommodated. The absence of an adjustable centering mechanism also introduced challenges in maintaining consistent axial alignment, particularly when mounting irregular or thin specimens. Misalignment during testing may have introduced unintended bending stresses, thus affecting result accuracy and test repeatability.

Another notable limitation was the lack of long-term performance assessment. The mechanical durability of the grip under repeated load cycles, clamping-unclamping operations, and prolonged laboratory use was not investigated. Phenomena such as thread wear, surface abrasion of the capstan drum, and bolt fatigue accumulation were outside the scope of this study, but they are critical considerations for routine or industrial usage.

All test setups, including specimen installation and preload application, were performed manually without torque-controlled instrumentation. As a result, operator-dependent variability could not be eliminated, potentially introducing inconsistencies in clamping force and boundary conditions across tests. Such variability is known to affect the reliability of force-displacement measurements in tensile experiments, especially for low-friction or compliant specimens.

Furthermore, the testing protocol was limited to monotonic axial loading within a moderate force range. The applied loads, while sufficient to evaluate initial performance and structural integrity, did not reach the upper thresholds of the Shimadzu testing system or the grip's theoretical design limits. Fatigue, dynamic, or impact loads were not considered. Thus, the design's response to extreme loading conditions remains unknown.

Environmental influences, such as humidity, temperature, and contamination—factors that significantly affect grip-sample friction—were also not addressed. All tests were conducted under controlled indoor conditions, limiting insight into how the system would perform in variable industrial or outdoor environments.

Finally, due to the budgetary and temporal constraints inherent to an undergraduate research project, the integration of advanced sensing technologies was not feasible. No in-situ instrumentation was included to measure slippage onset, contact pressure, or localized deformation. All observations were qualitative, based on visual inspections and post-failure evaluation.

8. CONCLUSION AND SUGGESTIONS FOR FUTURE STUDIES

8.1. Conclusions

This study set out to develop a reliable gripping solution for the tensile testing of flexible, rope-like materials, something that remains a common challenge in both academic and industrial testing environments. The Capstan Yarn Grip Apparatus designed and validated through this project offers a practical, structurally sound alternative to conventional wedge grips, particularly when dealing with specimens that are difficult to clamp without causing damage or slippage.

The journey began with a clearly defined problem: standard wedge grips often introduce localized stress concentrations and fail to securely hold soft or low-friction materials. To address this, the design focused on distributing load more evenly through frictional engagement, achieved by wrapping the specimen around a curved drum. After several design iterations, the final version was developed with a 300° wrap angle, a robust stainless steel body, and improved thread engagement for the clamping bolts. Throughout this process, stress concentration remained a key design concern and was minimized through both geometry and force path optimization.

To ensure the mechanical safety and performance of the apparatus, hand calculations were conducted to evaluate critical failure modes such as bolt shear and thread stripping. These were then validated through Finite Element Analysis (FEA), which showed consistent agreement with the analytical models. In particular, the simulation confirmed that the apparatus could safely sustain loading conditions up to the calculated limit, and that stress concentrations were well-managed—especially in areas around the bolt holes and clamping interfaces.

Experimental validation was carried out using the Shimadzu AGS-X Universal Testing Machine. A variety of materials—hemp rope, polypropylene cords, electrical cables, and steel wire ropes—were tested. Across all tests, the Capstan grip performed reliably. It prevented slippage, enabled clean failure in the gauge section, and produced smoother, more interpretable force-stroke curves compared to wedge grips. Notably, even high-strength steel wires were tested successfully without structural compromise, showing the grip's ability to handle a wide range of mechanical demands.

The design was also mindful of cost and practicality. Manufactured primarily from AISI 304 stainless steel and machined using industry-standard tools, the apparatus was built within a realistic budget of 12,500 TL. The timeline, spanning seven weeks from concept to testing, reflected an efficient yet thorough design and validation cycle, benefiting from both academic resources and industrial collaboration.

In conclusion, this project demonstrated that a well-engineered Capstan grip can significantly improve the reliability and accuracy of tensile testing for flexible materials. The apparatus meets both mechanical safety and functional requirements, and its performance was verified through a combination of theoretical, numerical, and experimental approaches. The emphasis on reducing stress concentrations proved essential, as it directly contributed to test repeatability and material integrity during high-load conditions.

Looking ahead, there are clear paths for improvement—such as integrating automation, modular features, or embedded sensors. However, even in its current form, the Capstan Yarn Grip Apparatus offers a strong foundation for future work and provides a practical, low-cost solution for mechanical testing labs dealing with non-rigid specimens.

8.2. Suggestions for Further Studies

Future research should seek to extend the applicability and performance characterization of the Capstan Yarn Grip Apparatus through methodological expansion, design optimization, and instrumentation enhancement.

First and foremost, subsequent studies should aim to evaluate the grip across a broader spectrum of material types. Including high-performance synthetic ropes, coated cables, and bio-compatible cords would provide more comprehensive validation and uncover material-specific challenges in frictional engagement or stress transfer. Particular attention should be given to ultra-thin or flat-profile specimens that are difficult to test using conventional grips.

The apparatus would also benefit from modular and adjustable architecture. Interchangeable capstan drums with varying radii and textures, combined with a centering and tensioning system, would greatly enhance usability and repeatability. This would allow fine-tuning of the contact interface based on the specimen's geometry and surface properties, minimizing off-axis loading and ensuring consistent frictional engagement.

Additionally, integrating sensing technologies such as strain gauges, load cells, and slip detection sensors would elevate the accuracy and resolution of the data obtained. Quantifying interfacial pressure distribution and monitoring micro-slippage in real time would provide deeper insight into failure mechanisms and improve correlation with analytical and finite element models.

Automating the pre-tensioning and clamping process through torque-limited or pneumatic systems could further reduce operator-induced inconsistencies. This would standardize boundary conditions across test runs, a critical requirement for high-precision mechanical testing.

Expanding the testing regime to include cyclic, fatigue, and creep tests would offer valuable data on the long-term mechanical reliability of the grip. Evaluating performance degradation over multiple loading cycles and under sustained stress conditions would simulate real-world scenarios more closely, particularly for applications in marine, elevator, or suspension systems.

Future experiments should also consider environmental sensitivity by conducting tests under varying humidity, temperature, and contamination conditions. Such conditions can alter the coefficient of friction at the grip-specimen interface and affect specimen behavior, thus impacting the grip's performance.

Finally, from a design optimization perspective, advanced simulation techniques such as nonlinear contact mechanics and topology optimization could be employed to improve material efficiency and minimize stress concentrations. Concurrently, aligning the system design with established testing standards (e.g., ASTM, ISO) and ensuring universal fixture compatibility would enhance the apparatus's potential for adoption in industrial and academic laboratories alike.

REFERENCES

1. ASTM D6775. (2021). *Standard test method for breaking strength and elongation of textile fabrics (strip method)*. ASTM International.

2. Coutellier, D., Lafaye, S., & Bailly, F. (2019). A review of gripping devices used for textile tensile testing. *Journal of Industrial Textiles*, 49(2), 199–218.

3. Friedrich, K., & Haufe, A. (2007). *Fracture mechanics of polymer composites*. Springer.

4. Hung, Y., Chen, J., & Tsai, Y. (2014). Analysis of Capstan grip design for tensile testing of flexible cords. *Experimental Techniques*, 38(4), 45–51.

5. Instron. (2023). *Capstan Grips for Flexible Materials*. Retrieved from https://www.instron.com

6. Lee, D., & Yang, C. (2017). Slip and failure analysis of synthetic rope grips. *Applied Mechanics and Materials*, 864, 101–107.

7. SDL Atlas. (2022). *Split Bollard Cord Grips*. Retrieved from https://sdlatlas.com/products/split-bollard-cord-grips-2kn

8. TestResources. (2023). *Capstan Rope & Thread Grips*. Retrieved from https://www.testresources.net/accessories/tensile-grips/capstan-grips

9. ANSYS Inc. (2023). *ANSYS Mechanical User's Guide, Release 2023 R1*. ANSYS Documentation Center. Retrieved from: https://www.ansys.com

10. Eytelwein, J. (1808). *Mechanik elastischer Körper*. (Referenced in derivation of the Capstan equation).

11. SolidWorks. (2023). *SOLIDWORKS Help: Assemblies and Part Modeling Guide*. Dassault Systèmes. Retrieved from: https://www.solidworks.com

12. Trapezium X Software. (2022). *Shimadzu Testing System User Manual*. Shimadzu Corporation. Retrieved from: https://www.shimadzu.com/an/products/testing/

13. ISO 7500-1. (2018). *Metallic materials – Calibration and verification of static uniaxial testing machines – Part 1: Tension/compression testing machines*. International Organization for Standardization.

14. ISO 898-1. (2013). *Mechanical properties of fasteners made of carbon steel and alloy steel – Part 1: Bolts, screws and studs with specified property classes – Coarse thread and fine pitch thread*. International Organization for Standardization.

15. Bickford, J. H. (2008). *An Introduction to the Design and Behavior of Bolted Joints* (4th ed.). CRC Press.→ Includes detailed derivations for thread stripping, tensile and shear design, and joint preload analysis.

16. Shigley, J. E., Mischke, C. R., & Budynas, R. G. (2011). *Shigley's Mechanical Engineering Design* (9th ed.). McGraw-Hill. → Contains standard bolt strength tables, thread geometry, shear stress calculations, and design equations for eccentric loading.

17. ISO 898-2. (2012). *Mechanical properties of fasteners made of carbon steel and alloy steel – Part 2: Nuts with specified property classes – Coarse thread and fine pitch thread*. International Organization for Standardization.

18. ASME B1.1. (2003). *Unified Inch Screw Threads (UN and UNR Thread Form)*. The American Society of Mechanical Engineers. → Reference for standard thread geometry used in thread stripping area calculations.

19. Machinery's Handbook. (2020). *30th Edition*. Industrial Press. → Practical formulas, thread dimensions, bolt capacity charts, and material properties—widely used in industry.

APPENDICES

Raw testing data is available as soft copy.

Figures A1 through **A5** illustrate the first Capstan grip design from multiple angles including front, right, back, and isometric views. This initial version lacked symmetry and had slender clamping arms, making it prone to structural deflection and eccentric loading under tensile forces.

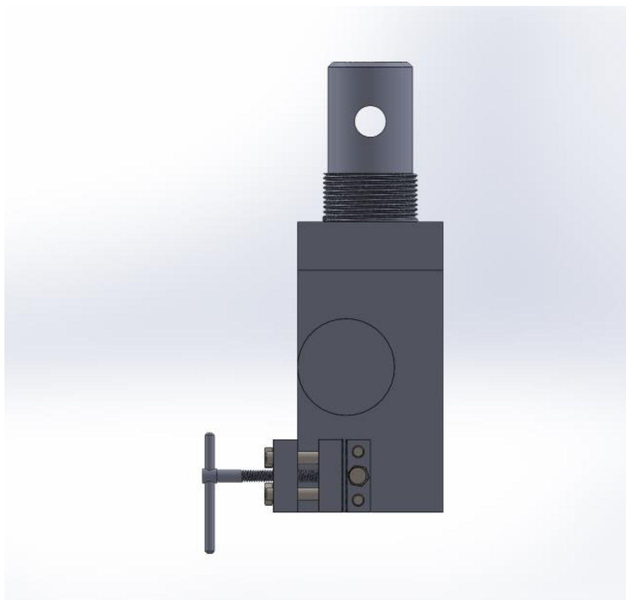

Figure A 1 - First Design - SolidWorks Front View

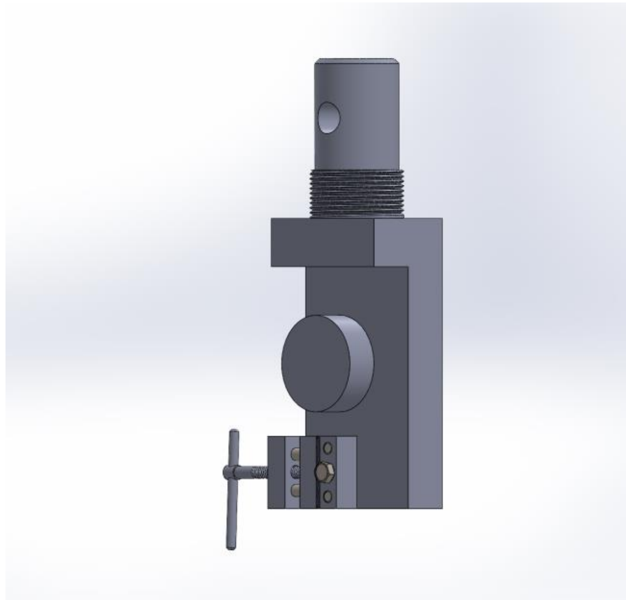

Figure A 2 - First Design - SolidWorks Isometric View

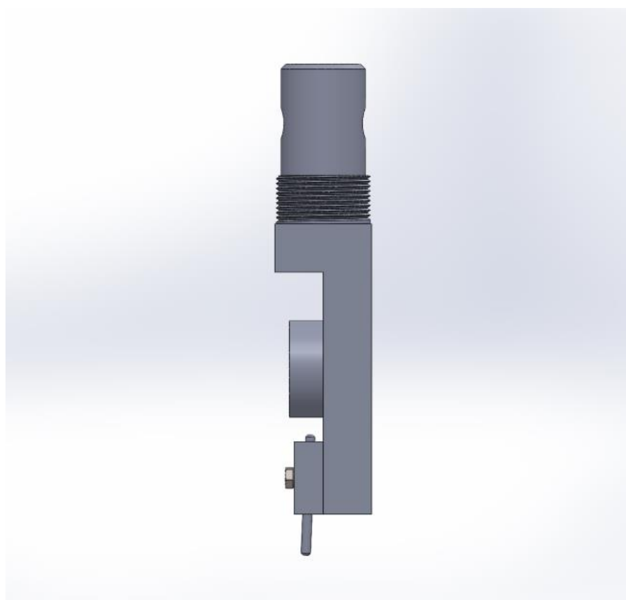

Figure A 3 - First Design - SolidWorks Right View

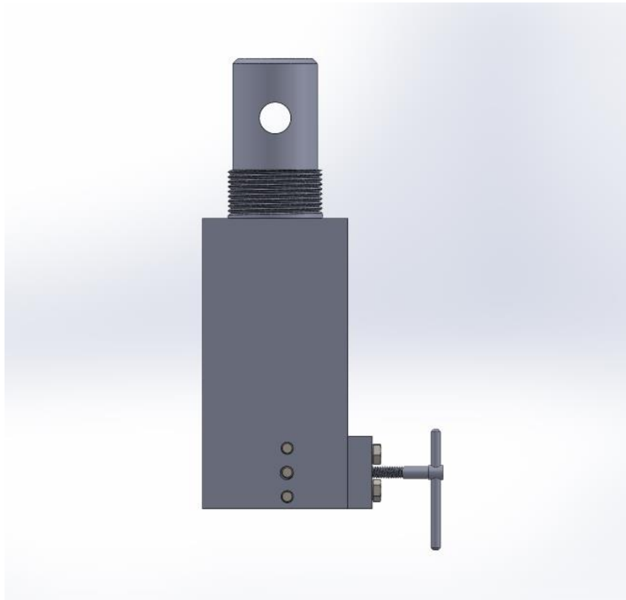

Figure A 4 - First Design - SolidWorks Back View

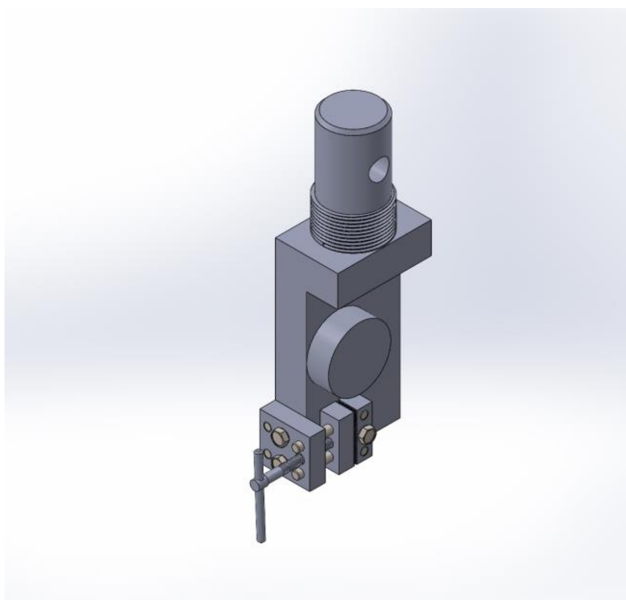

Figure A 5 - First Design - SolidWorks Isometric View from Left

Figures A6 to **A9** show the second design iteration of the Capstan grip. This version incorporated thicker structural sections and a more enclosed geometry. While improvements were made, the arms remained too narrow, and load transfer was still unbalanced, prompting further optimization.

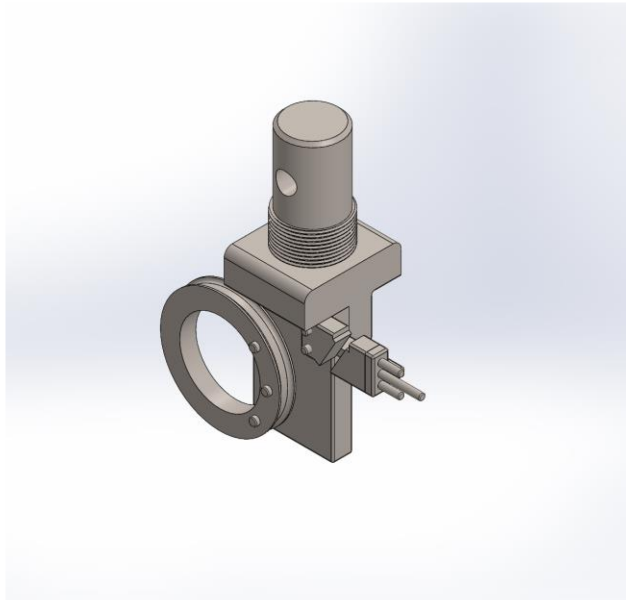

Figure A 6 - Second Design – SolidWorks Isometric View

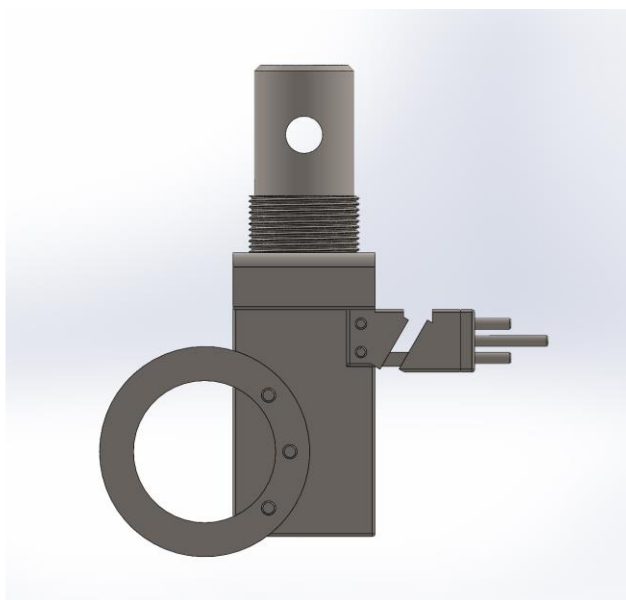

Figure A 7 - Second Design – SolidWorks Front View

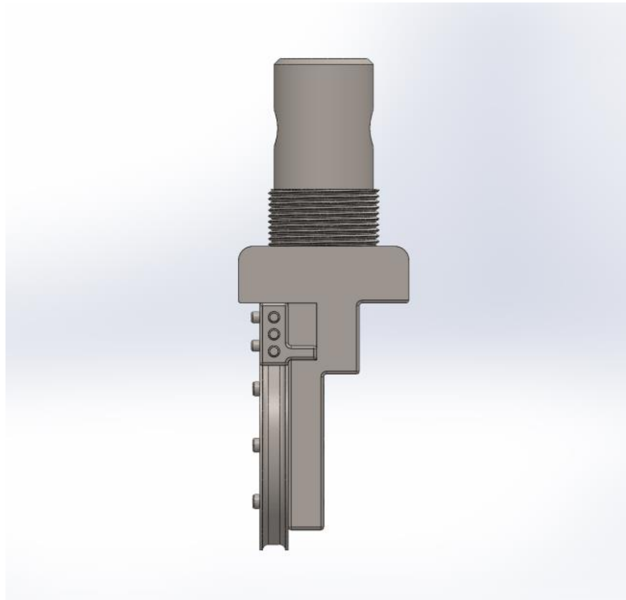

Figure A 8 - Second Design – SolidWorks Right View

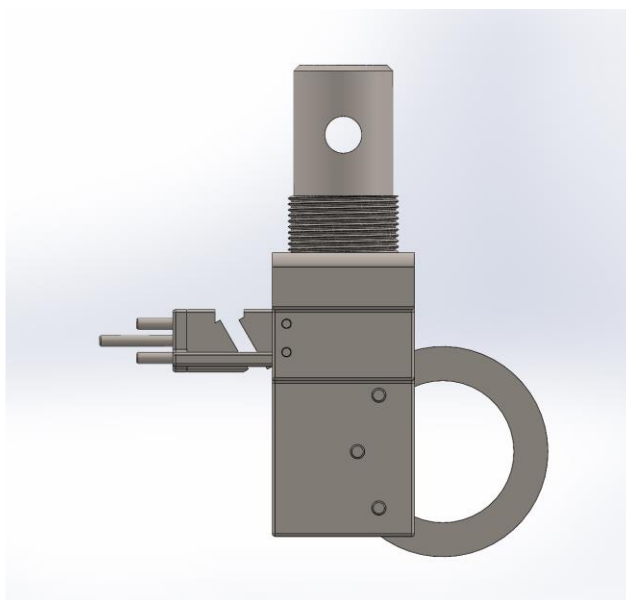

Figure A 9 - Second Design – SolidWorks Back View

Figure A10 presents the final isometric view of the optimized Capstan grip. This design achieves structural symmetry, improved stress distribution, and increased rigidity through enhanced clamp geometry and reinforcement features.

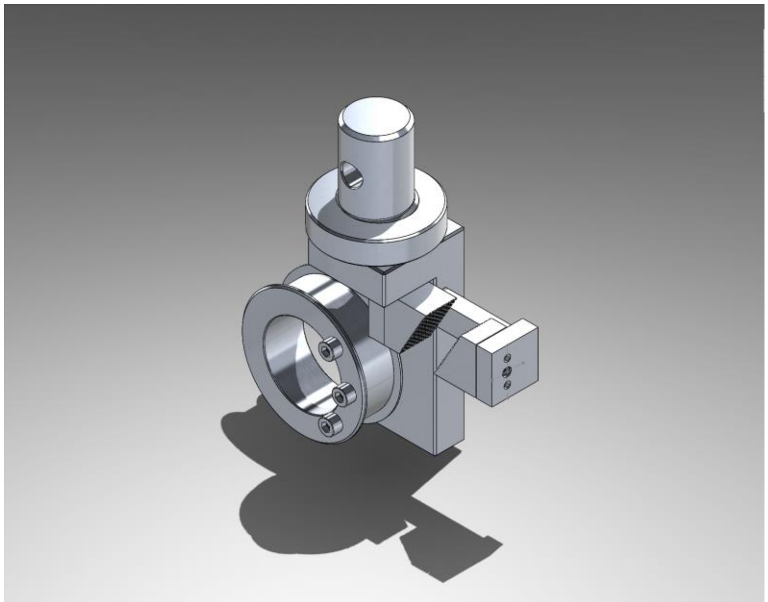

Figure A 10 - Final Design - SolidWorks Isometric View

Figures A11 through **A16** provide comprehensive views of the final Capstan grip design from multiple orientations, including front, right, back, and isometric perspectives. These views confirm the improved geometry, symmetrical body structure, and the presence of robust clamping features to resist eccentric loads.

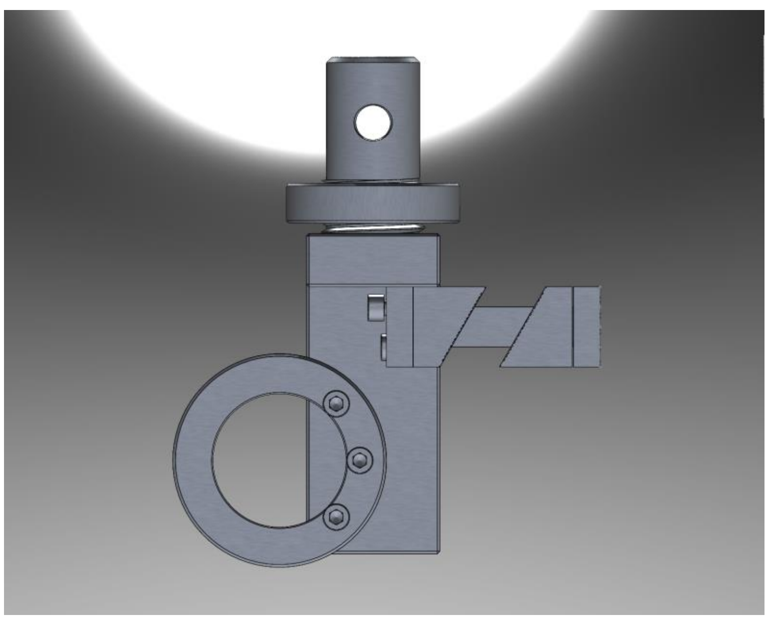

Figure A 11 - Final Design – SolidWorks Front View

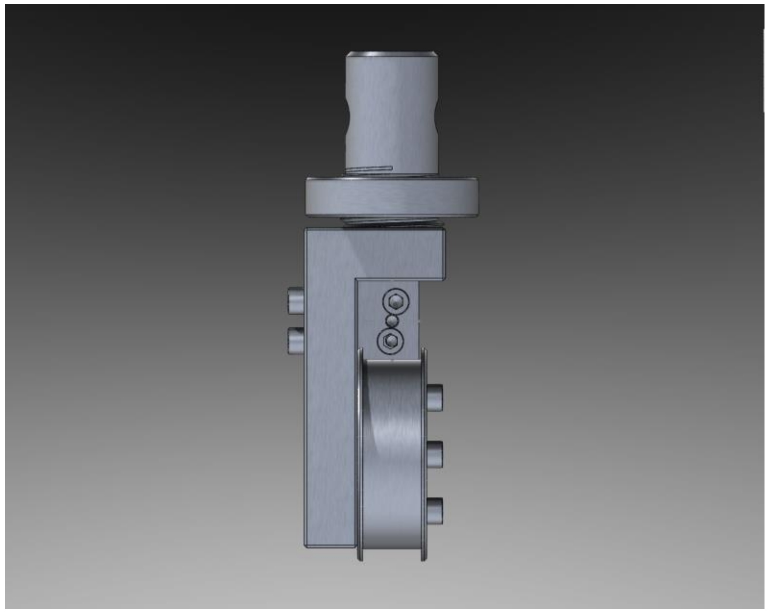

Figure A 12 - Final Design – SolidWorks Left View

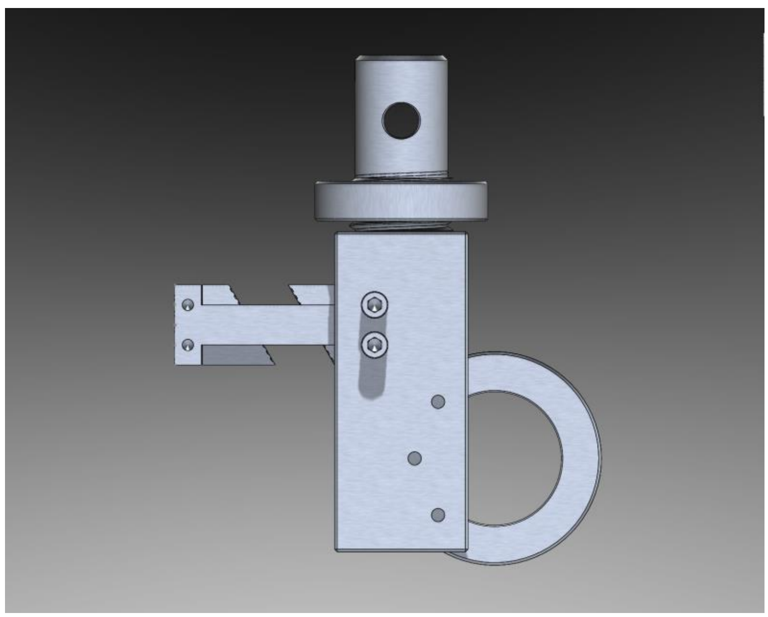

Figure A 13 - Final Design – SolidWorks Back View

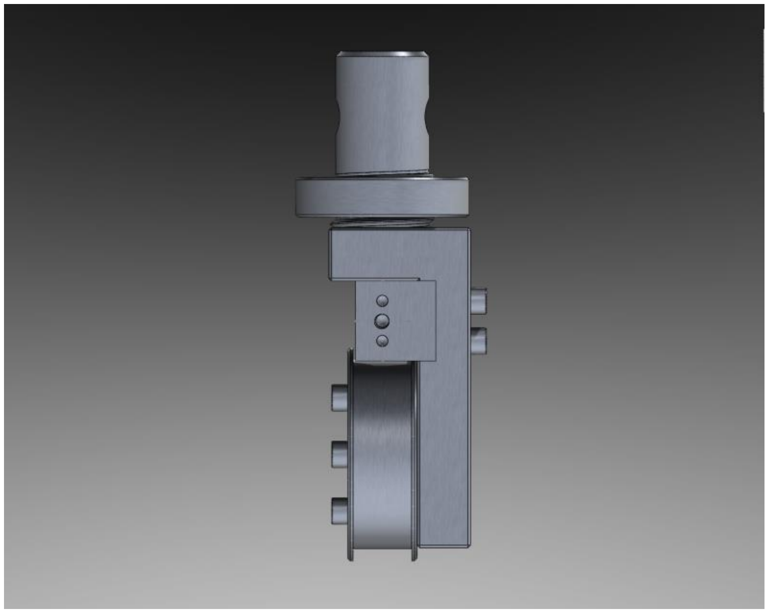

Figure A 14 - Final Design – SolidWorks Right View

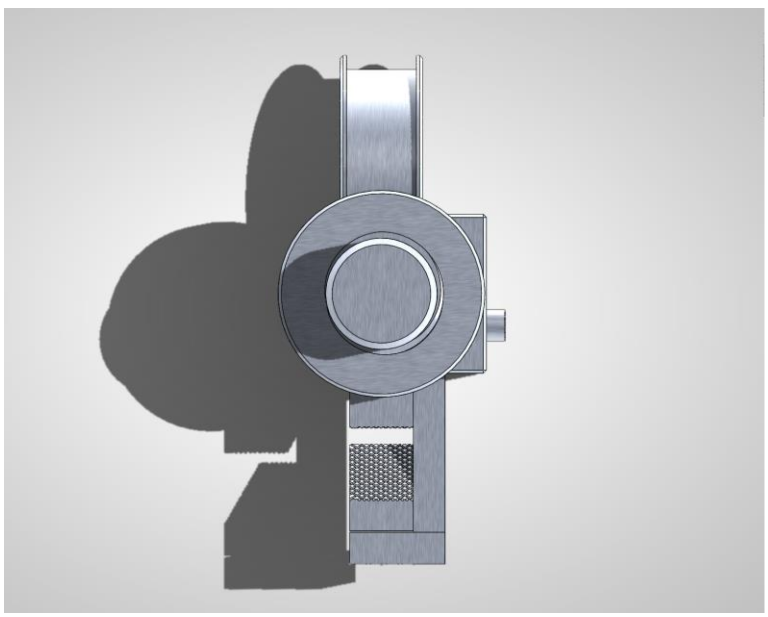

Figure A 15 - Final Design – SolidWorks Top View

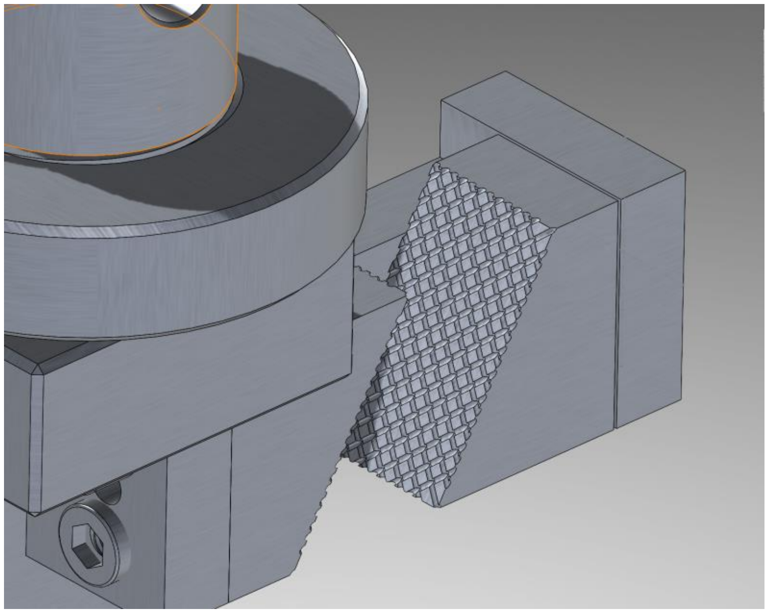

Figure A 16 - Final Design – SolidWorks Clamp Jaw Close Up View

Table A1 presents the fundamental mechanical properties of bolts according to ISO 898-1. These values are used to assess bolt suitability for tensile and shear loading in the grip structure.

Table A 1 *- ISO 898-1 - Mechanical and physical properties of bolts*

No.	Mechanical or physical property		Property class 4.6	4.8	5.6	5.8	6.8	8.8 d u 16 mm [a]	8.8 d > 16 mm [b]	9.8 d u 16 mm	10.9	12.9/ 12.9
1	Tensile strength, R_m, MPa	nom. [c]	400		500		600	800		900	1 000	1 200
		min.	400	420	500	520	600	800	830	900	1 040	1 220
2	Lower yield strength, R_{eL} [d], MPa	nom. [c]	240	—	300	—	—	—	—	—	—	—
		min.	240	—	300	—	—	—	—	—	—	—
3	Stress at 0,2 % non-proportional elongation, $R_{p0,2}$, MPa	nom. [c]	—	—	—	—	—	640	640	720	900	1 080
		min.	—	—	—	—	—	640	660	720	940	1 100
4	Stress at 0,0048 d non-proportional elongation for full-size fasteners, R_{pf}, MPa	nom. [c]	—	320	—	400	480	—	—	—	—	—
		min.	—	340 [e]	—	420 [e]	480 [e]	—	—	—	—	—
	Stress under proof load, S_p [f], MPa	nom.	225	310	280	380	440	580	600	650	830	970

5	Proof strength ratio	$S_{p,nom}/R_{eL\,min}$ or $S_{p,nom}/R_{p0,2\,min}$ or $S_{p,nom}/R_{pf\,min}$	0,94	0,91	0,93	0,90	0,92	0,91	0,91	0,90	0,88	0,88
6	Percentage elongation after fracture for machined test pieces, A, %	min.	22	—	20	—	—	12	12	10	9	8
7	Percentage reduction of area after fracture for machined test pieces, Z, %	min.	—					52		48	48	44
8	Elongation after fracture for full-size fasteners, A_f (see also Annex C)	min.	—	0,24	—	0,22	0,20	—	—	—	—	—
9	Head soundness		No fracture									

Table A2 expands upon ISO 898-1 specifications, including hardness ratings, elongation limits, and proof loads, which are critical for thread stripping and clamping force calculations.

***Table A 2** - ISO 898-1 - Mechanical and physical properties of bolts (Continued)*

No.	Mechanical or physical property		Property class									
			4.6	4.8	5.6	5.8	6.8	8.8		9.8	10.9	12.9/ <u>12.9</u>
								d u 16 mm [a]	d > 16 mm [b]	d u 16 m m		
10	Vickers hardness, HV F W 98 N	min.	120	130	155	160	190	250	255	290	320	385
		max.	220 [g]				250	320	335	360	380	435
11	Brinell hardness, HBW F = 30 D^2	min.	114	124	147	152	181	238	242	276	304	366
		max.	209 [g]				238	304	318	342	361	414
12	Rockwell hardness, HRB	min.	67	71	79	82	89	—				
		max.	95,0 [g]				99,5	—				
	Rockwell hardness, HRC	min.	—					22	23	28	32	39
		max.	—					32	34	37	39	44
13	Surface hardness, HV 0,3	max.	—					h			h, i	h, j
14	Height of non-decarburized thread zone, E, mm	min.	—					$^{1}/_{2}H_1$			$^{2}/_{3}H_1$	$^{3}/_{4}H_1$
	Depth of complete decarburization in the thread, G, mm	max.	—					0,015				
15	Reduction of hardness after retempering, HV	max.	—					20				

16	Breaking torque, M_B, N·m	min.	—					in accordance with ISO 898-7				
17	Impact strength, K_V [k, l], J	min.	—		27	—		27	27	27	27	m
18	Surface integrity in accordance with		ISO 6157-1 [n]									ISO 6157-3

[a] Values do not apply for structural bolting.

[b] For structural bolting d W M12.

[c] Nominal values are specified only for the purpose of the designation system for property classes. See Clause 5.

[d] In cases where the lower yield strength R_{eL} cannot be determined, it is permissible to measure the stress at 0,2 % non-proportional elongation $R_{p0,2}$.

[e] For the property classes 4.8, 5.8 and 6.8 the values for $R_{pf\ min}$ are under investigation. The present values are given for calculation of the proof stress ratio only. They are not test values.

[f] Proof loads are specified in Tables 5 and 7.

[g] Hardness determined at the end of a fastener shall be 250 HV, 238 HB or 99,5 HRB maximum.

[h] Surface hardness shall not be more than 30 Vickers points above the measured core hardness of the fastener when determination of both surface hardness and core hardness are carried out with HV 0,3.

[i] Any increase in hardness at the surface which indicates that the surface hardness exceeds 390 HV is not acceptable.

[j] Any increase in hardness at the surface which indicates that the surface hardness exceeds 435 HV is not acceptable.

[k] Values are determined at a test temperature of −20 °C, see 9.14.

[l] Applies to d W 16 mm.

[m] Value for K_V is under investigation.

[n] Instead of ISO 6157-1, ISO 6157-3 may apply by agreement between the manufacturer and the purchaser.

Table A3 lists the minimum ultimate tensile loads for various metric bolts. These serve as reference points to ensure safety margins in the grip's bolted joints.

Table A 3 *- ISO 898-1 - Minimum Ultimate Tensile Loads*

Thread [a] d	Nominal stress area $A_{s,nom}$ [b] mm^2	Property class								
		4.6	4.8	5.6	5.8	6.8	8.8	9.8	10.9	12.9/<u>12.9</u>
		Minimum ultimate tensile load, $F_{m\ min}$ ($A_{s,\ nom} \times R_{m,\ min}$), N								
M3	5,03	2 010	2 110	2 510	2 620	3 020	4 020	4 530	5 230	6 140
M3,5	6,78	2 710	2 850	3 390	3 530	4 070	5 420	6 100	7 050	8 270
M4	8,78	3 510	3 690	4 390	4 570	5 270	7 020	7 900	9 130	10 700
M5	14,2	5 680	5 960	7 100	7 380	8 520	11 350	12 800	14 800	17 300
M6	20,1	8 040	8 440	10 000	10 400	12 100	16 100	18 100	20 900	24 500
M7	28,9	11 600	12 100	14 400	15 000	17 300	23 100	26 000	30 100	35 300
M8	36,6	14 600 [c]	15 400	18 300 [c]	19 000	22 000	29 200 [c]	32 900	38 100 [c]	44 600
M10	58	23 200 [c]	24 400	29 000 [c]	30 200	34 800	46 400 [c]	52 200	60 300 [c]	70 800
M12	84,3	33 700	35 400	42 200	43 800	50 600	67 400 [d]	75 900	87 700	103 000
M14	115	46 000	48 300	57 500	59 800	69 000	92 000 [d]	104 000	120 000	140 000
M16	157	62 800	65 900	78 500	81 600	94 000	125 000 [d]	141 000	163 000	192 000
M18	192	76 800	80 600	96 000	99 800	115 000	159 000	—	200 000	234 000
M20	245	98 000	103 000	122 000	127 000	147 000	203 000	—	255 000	299 000
M22	303	121 000	127 000	152 000	158 000	182 000	252 000	—	315 000	370 000

M24	353	141 000	148 000	176 000	184 000	212 000	293 000	—	367 000	431 000
M27	459	184 000	193 000	230 000	239 000	275 000	381 000	—	477 000	560 000
M30	561	224 000	236 000	280 000	292 000	337 000	466 000	—	583 000	684 000
M33	694	278 000	292 000	347 000	361 000	416 000	576 000	—	722 000	847 000
M36	817	327 000	343 000	408 000	425 000	490 000	678 000	—	850 000	997 000
M39	976	390 000	410 000	488 000	508 000	586 000	810 000	—	1 020 000	1 200 000

[a] Where no thread pitch is indicated in a thread designation, coarse pitch is specified.

[b] To calculate $A_{s,nom}$, see 9.1.6.1.

[c] For fasteners with thread tolerance 6az according to ISO 965-4 subject to hot dip galvanizing, reduced values in accordance with ISO 10684:2004, Annex A, apply.

[d] For structural bolting 70 000 N (for M12), 95 500 N (for M14) and 130 000 N (for M16).

Table A4 shows the raw tensile test data provided by the DARHAN company for their steel wire products. These values were used to compare with internal test results and validate the performance of the Capstan grip.

Table A 4 *- DARHAN - Steel Wire Tensile Test Results*

Desk	Product name	Test Nr.	Test Position	Reached Load (N)	Reached Load (kgf)	Result
1	SAS 2.0 Seismic Bracing Cable Set, 2.0 mm	1	0°	3706	377	OK
		2	0°	3780	385	OK
		3	0°	3897	397	OK
2	SAS 2.4 Seismic Bracing Cable Set, 2.4 mm	1	0°	4741	483	OK
		2	0°	5079	517	OK
		3	0°	4753	484	OK
3	SAS 3.0 Seismic Bracing Cable Set, 3.0 mm	1	0°	7383	752	OK
		2	0°	7322	746	OK
		3	0°	7288	743	OK
4	SAS 4.0 Seismic Bracing Cable Set, 4.0 mm	1	0°	11093	1130	OK
		2	0°	11188	1140	OK
		3	0°	11144	1136	OK
5	SAS 5.0 Seismic Bracing Cable Set, 5.0 mm	1	0°	18894	1926	OK
		2	0°	18724	1908	OK
		3	0°	18851	1922	OK
6	SAS 6.0 Seismic Bracing Cable Set, 6.0 mm	1	0°	25743	2624	OK
		2	0°	24547	2502	OK
		3	0°	26694	2721	OK

Figure A17 documents the tensile test setup provided by the DARHAN company for steel wire specimens. It validates external testing procedures and material behavior under industry-standard conditions.

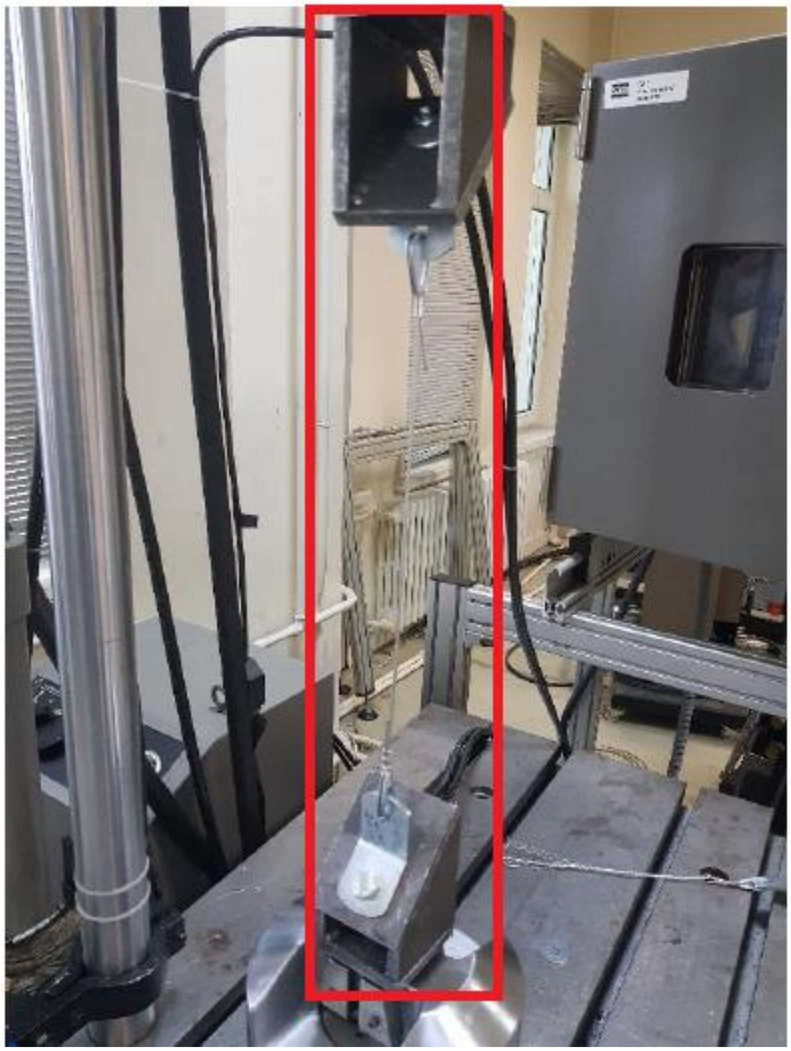

Figure A 17 - DARHAN - Steel Wire Test Environment

Figure A18 shows the typical Allen bolt used in the Capstan grip apparatus. These fasteners were analyzed for thread stripping and shear strength under eccentric loading conditions.

Figure A 18 - Example Alen Bolt

Figures A19 through **A43** display various specimens after tensile testing using Capstan and Wedge grips. The images capture failure modes, slippage marks, necking, and fracture locations across a variety of materials such as **hemp rope**, **electrical cable**, **polypropylene**, and **steel wire**. These figures help visualize the effectiveness of each grip design in securing the specimen and ensuring valid mechanical failure within the gauge length.

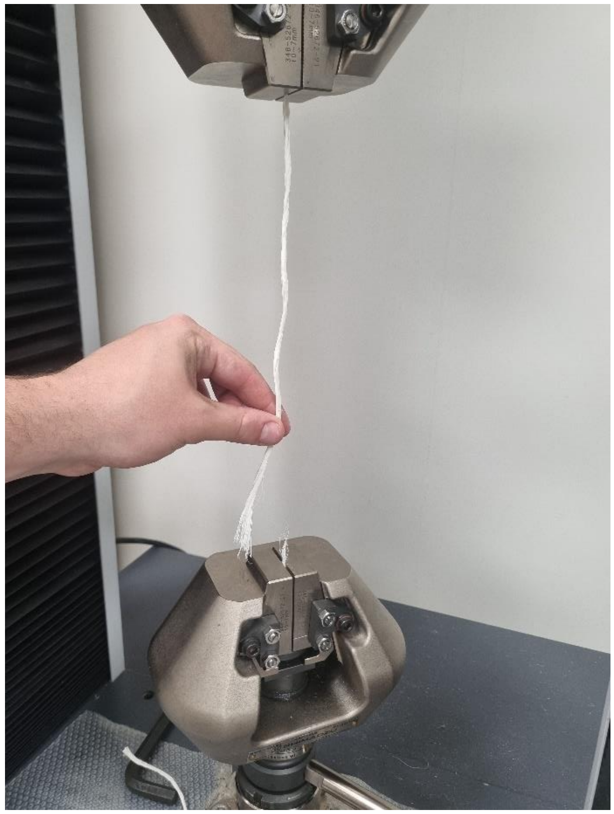

Figure A 19 - 1.5mm PP - Wedge Grip Test Result - 2

Figure A 20 - 1.5mm PP - Wedge Grip Test Result

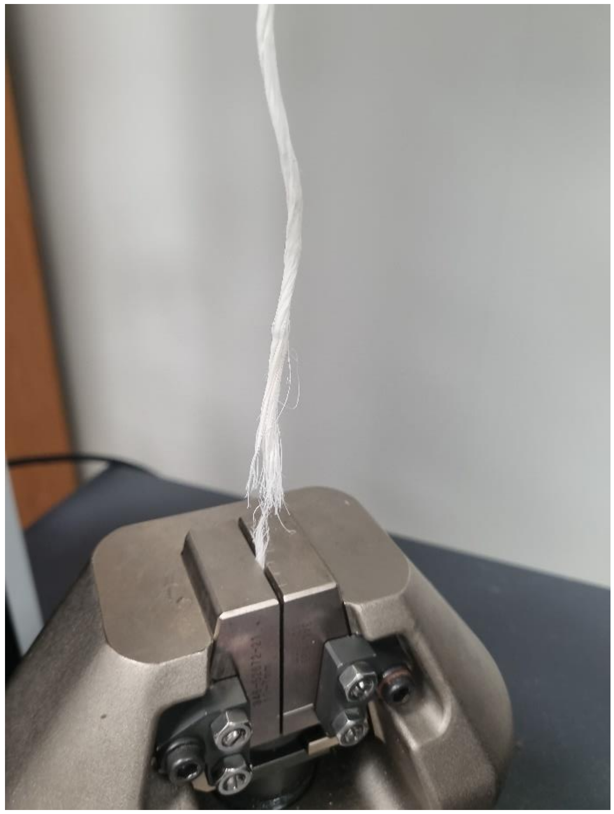

Figure A 21 - 1.5mm PP – Wedge Grip Test Result Close Up

Figure A 22 - 1.5mm PP – Capstan Test Result

Figure A 23 - 1.5mm PP – Capstan Test Result Close Up

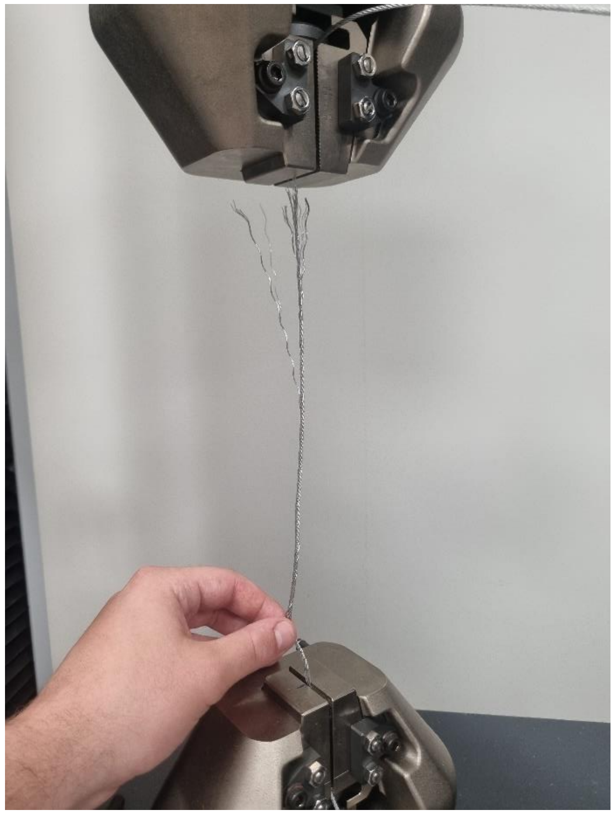

Figure A 24 - 2mm Steel Wire – Wedge Grip Test Result

Figure A 25 - 6mm Hemp Rope – Wedge grip test close up

Figure A 26 - 6mm Hemp Rope – Wedge Grip Test

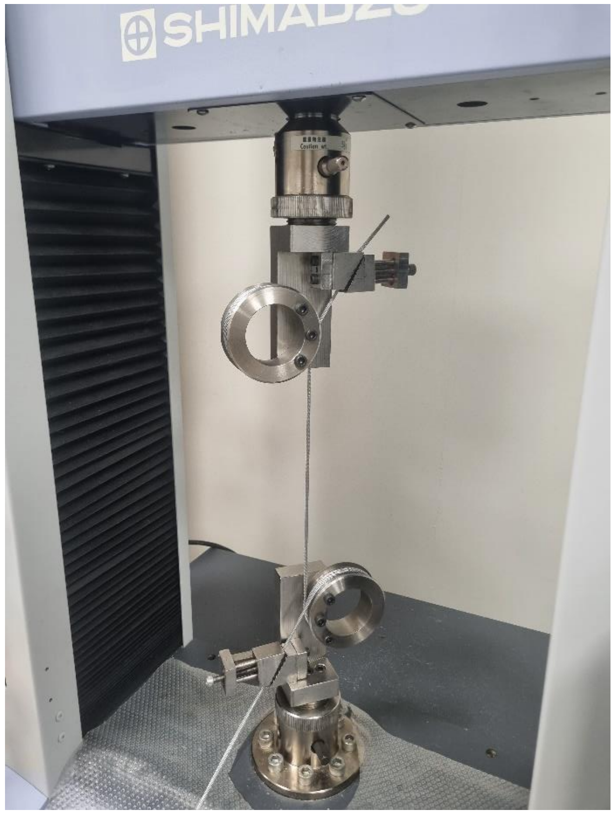

Figure A 27 - 2mm Steel Wire – Before the Capstan Test

Figure A 28 - 2mm Steel Wire – Capstan Test Result Wide Angle

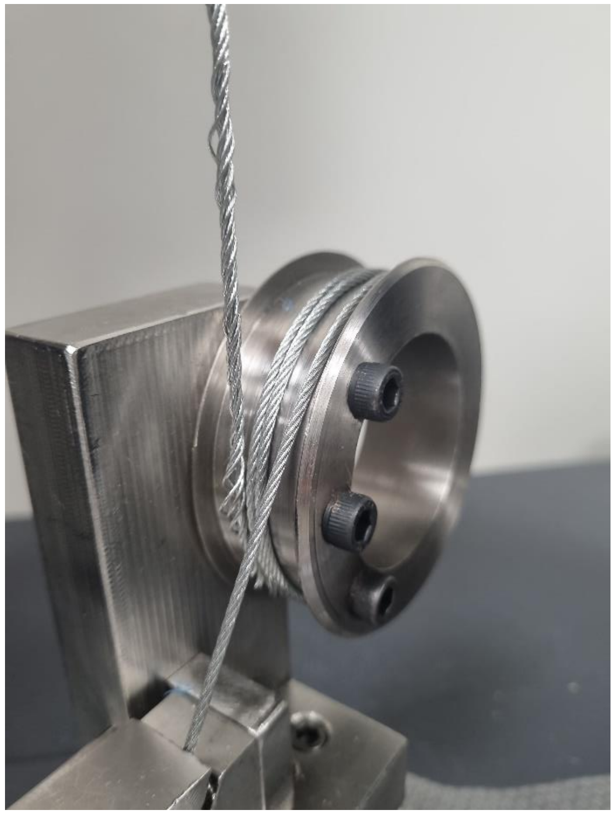

Figure A 29 - 2mm Steel Wire -Capstan Test Result Close up bottom

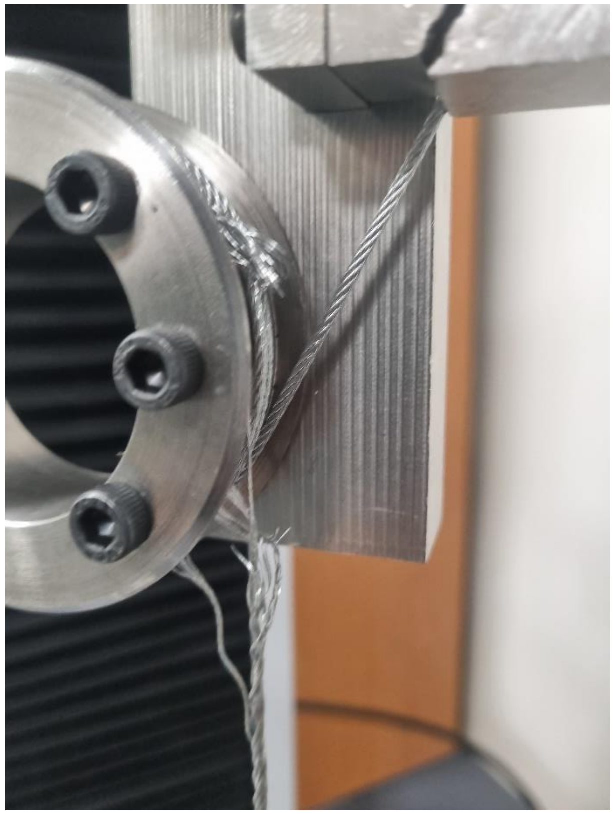

Figure A 30 - 2mm Steel Wire – Capstan Test Result Close up upper

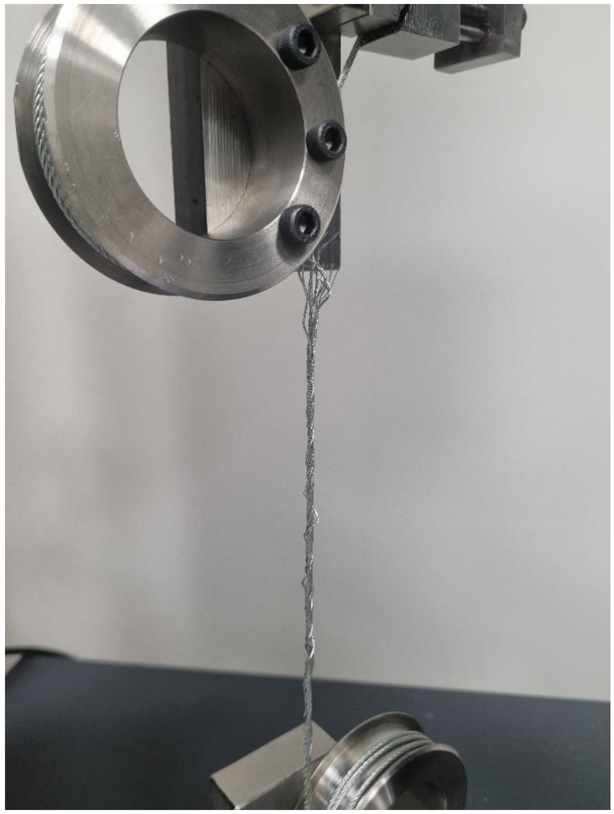

Figure A 31 - 2mm Steel Wire – Capstan Test Result

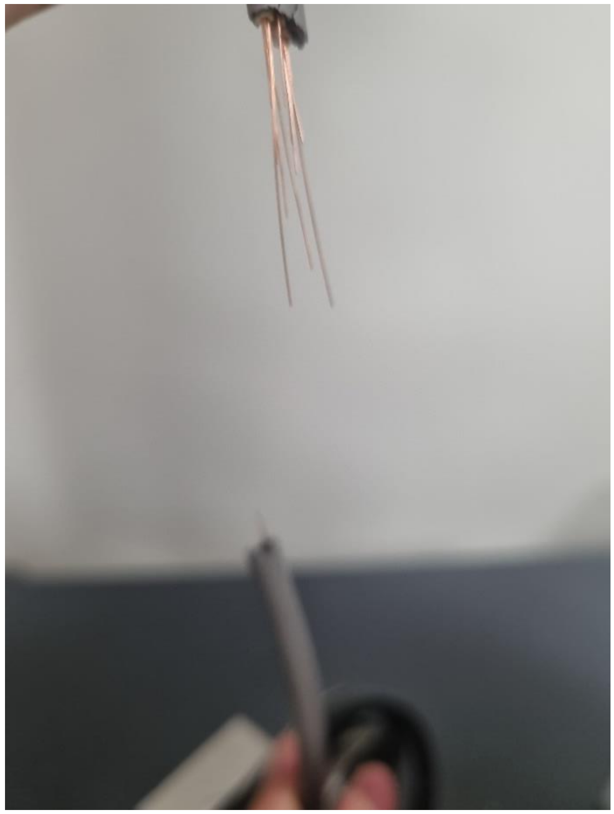

Figure A 32 - 5mm Electrical Cable – Copper wires after the test

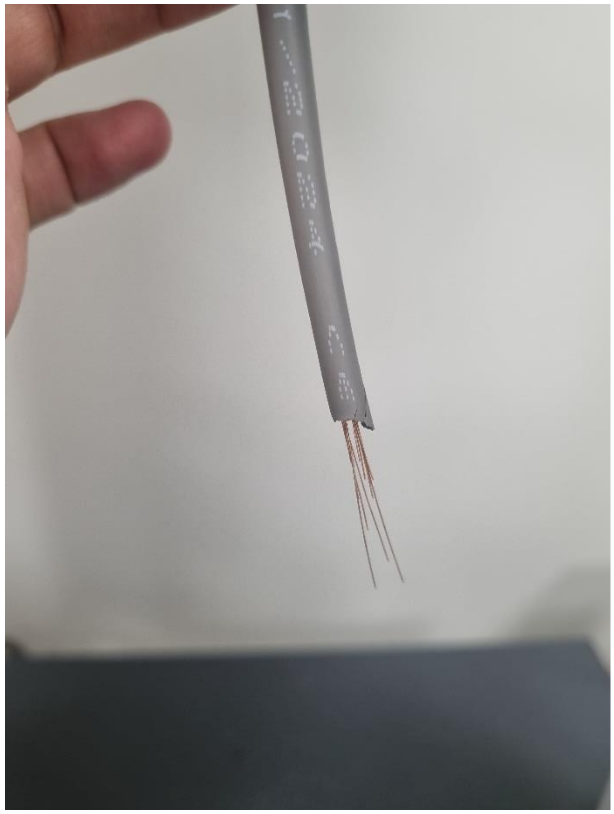

Figure A 33 - 5mm Electrical Cable – After The Test

Figure A 34 - 5mm Electrical Cable – Test Result Side View

Figure A 35 - 5mm Electrical Cable – Test Result

Figure A 36 - 2.5mm PP – Test Result

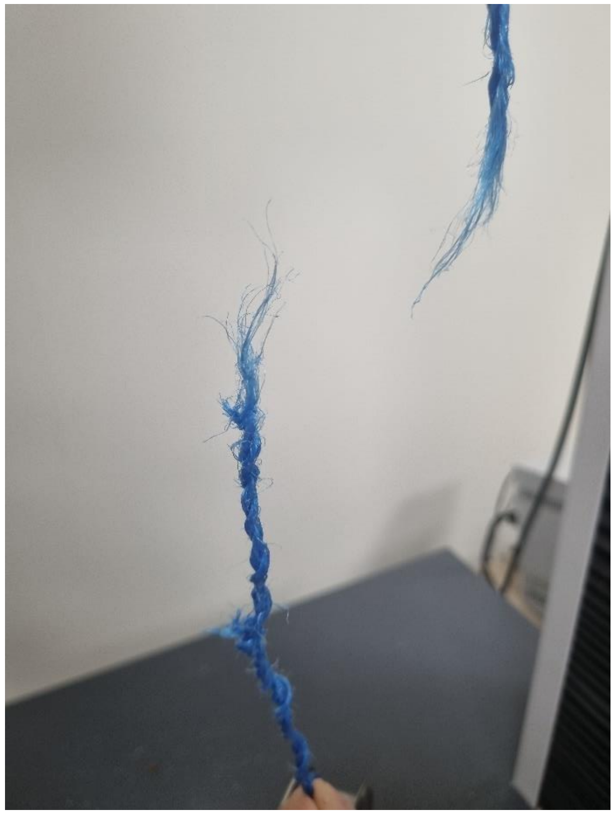

Figure A 37 - 2.5mm PP – Capstan Test Result Close up

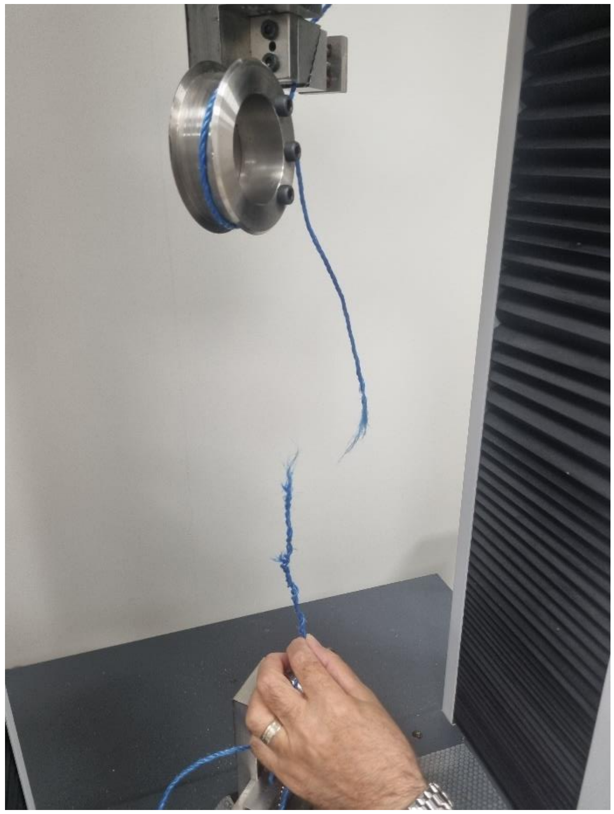

Figure A 38 - 2.5mm PP – Capstan Test Result

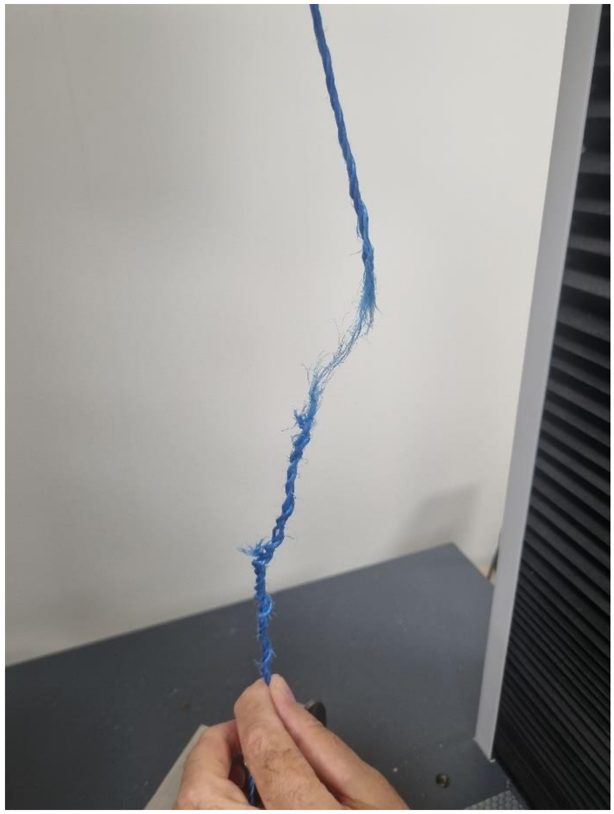

Figure A 39 - 2.5mm PP – Capstan Failure Zone Close Up

Figure A 40 - 6mm Hemp Rope – Test Result Close up

Figure A 41 - 5mm Hemp Rope - Test Result

Figure A 42 - 6mm Hemp Rope – Test Result Close up

Figure A 43 - 5mm Hemp Rope – Before Test

Figure A44 illustrates the finite element mesh applied to the full Capstan grip assembly. A finer mesh was generated near bolt holes and contact surfaces to accurately capture localized stress distributions.

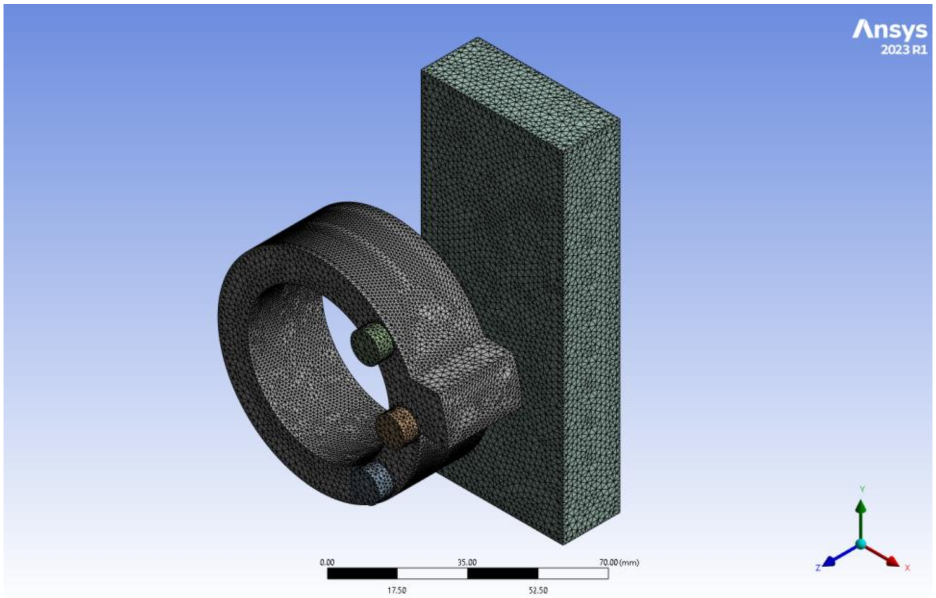

Figure A 44 - ANSYS - MESH Preview of Whole Body

Figure A45 provides a close-up of the meshing around the bolt region. The refined triangular elements help ensure accurate shear and tensile stress evaluations where load transfer occurs.

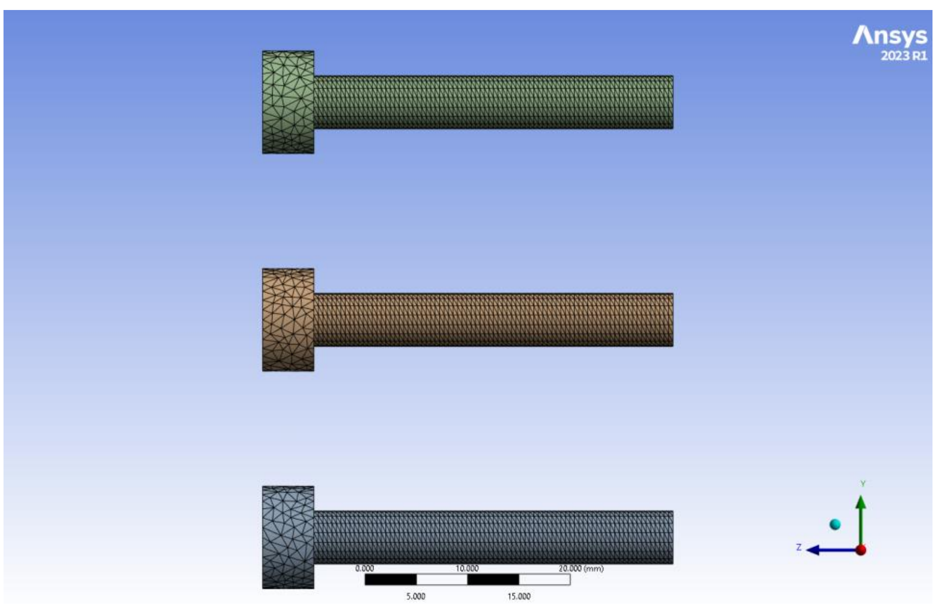

Figure A 45 - ANSYS - MESH Preview of Bolts

Figure A46 presents an isometric view of the complete meshed model. The visualization confirms that mesh density transitions smoothly from critical to non-critical regions, ensuring solution efficiency without compromising accuracy.

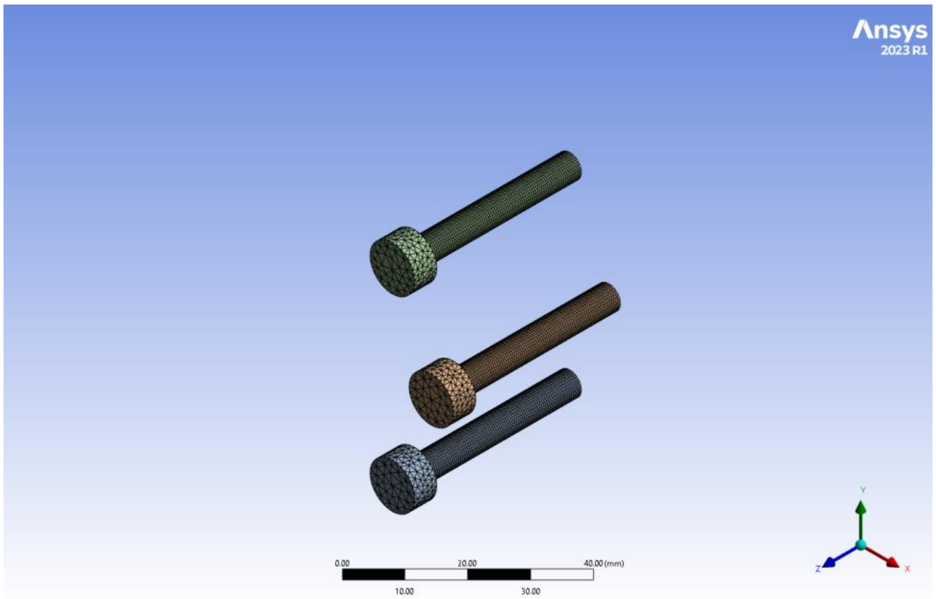

Figure A 46 - ANSYS - MESH Preview of Bolts - Iso View

Figure A47 presents the von Mises stress distribution across the Capstan grip assembly under a 7.1 kN load. Stress concentrations are primarily located near the bolt holes and the contact interface between the capstan drum and the body, indicating initial areas of concern under lower loading.

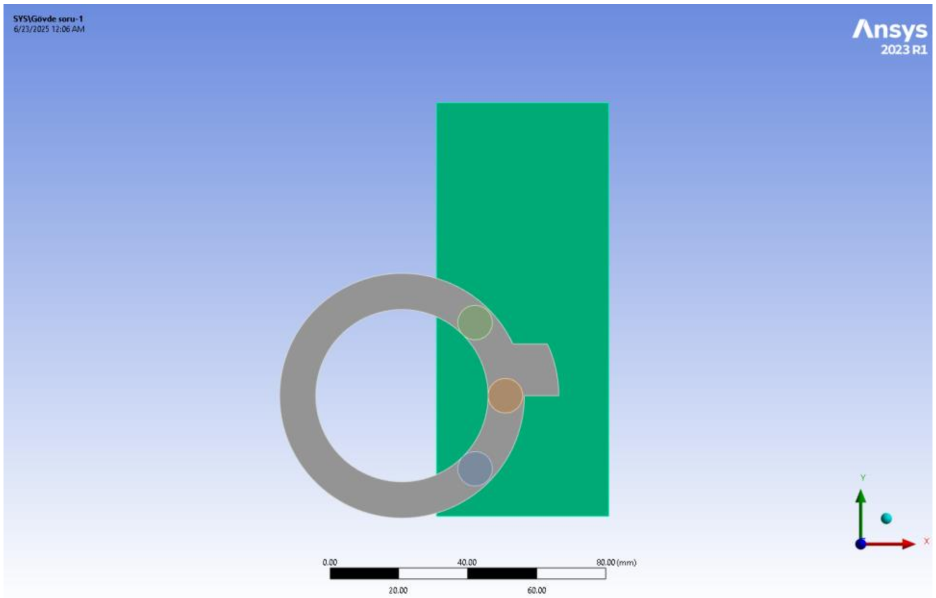

Figure A 47 - ANSYS - Simplified Model for Simulation – Front View

Figure A48 shows the stress distribution under a 14 kN applied force. Compared to 7.1 kN, the stress magnitudes have increased proportionally, with elevated concentrations around the clamping bolt regions and capstan bore holes, nearing material limits.

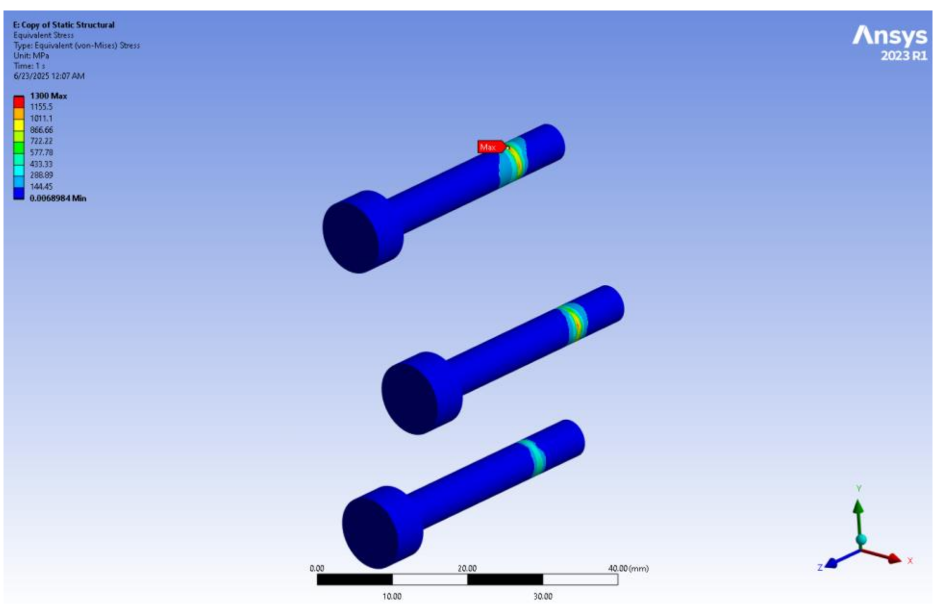

Figure A 48 - ANSYS - 7.1kN von-Mises stress

Figure A49 provides a close-up view of the capstan hole under 7.1 kN loading. The stress is uniformly distributed around the inner curvature, suggesting good contact transfer and no abrupt discontinuities at this load level.

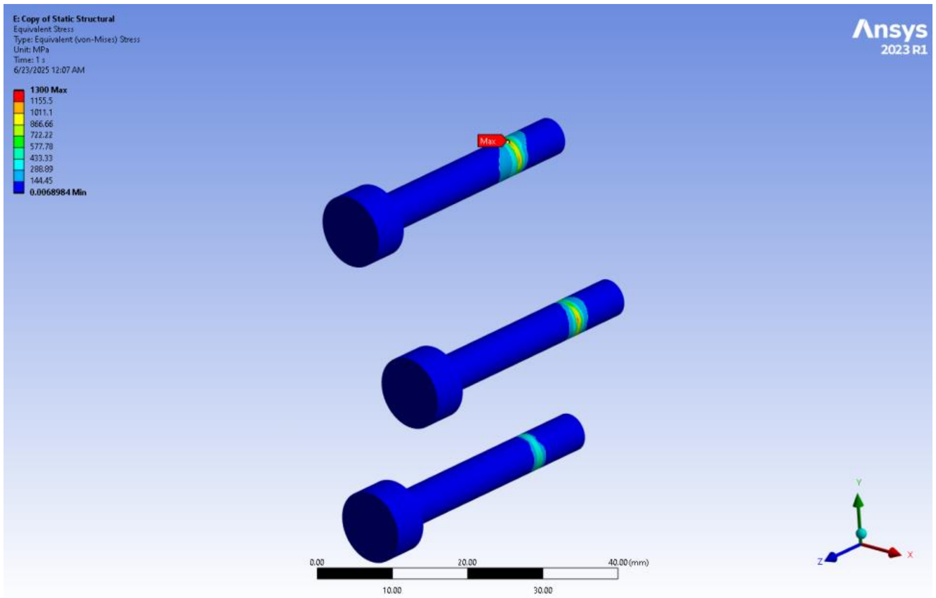

Figure A 49 - ANSYS - 14kN von-Mises stress

Figure A50 depicts localized stress behavior at the capstan hole with 14 kN loading. The intensity increase reveals stress concentration at the curved transition regions, indicating potential failure initiation zones under high load.

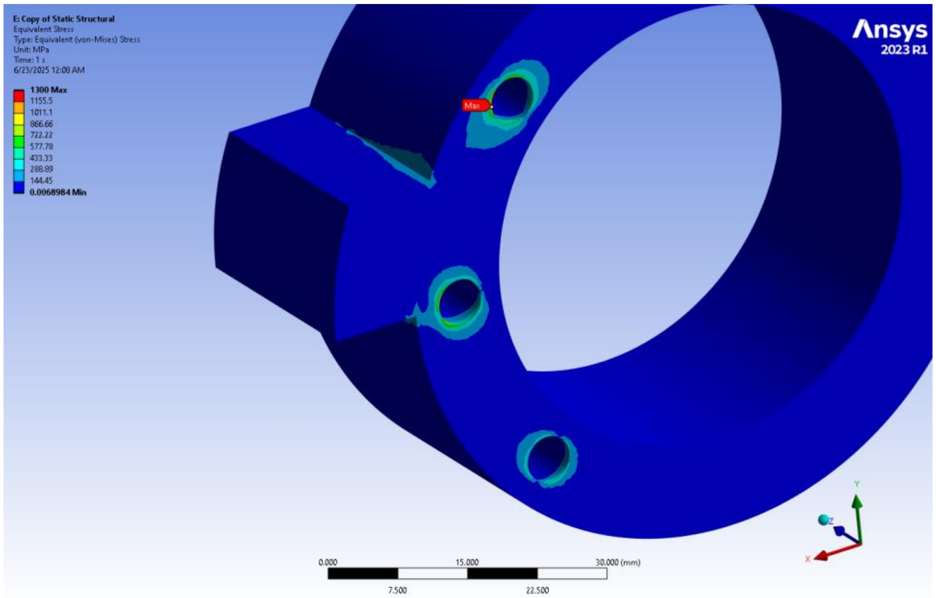

Figure A 50 - ANSYS - 7.1kN CAPSTAN HOLE CLOSEUP - von-Mises stress

Figure A51 highlights the body hole region under 7.1 kN of tensile loading. The stress distribution remains moderate, with values well below the yield limit, suggesting safe performance in early stages of load application.

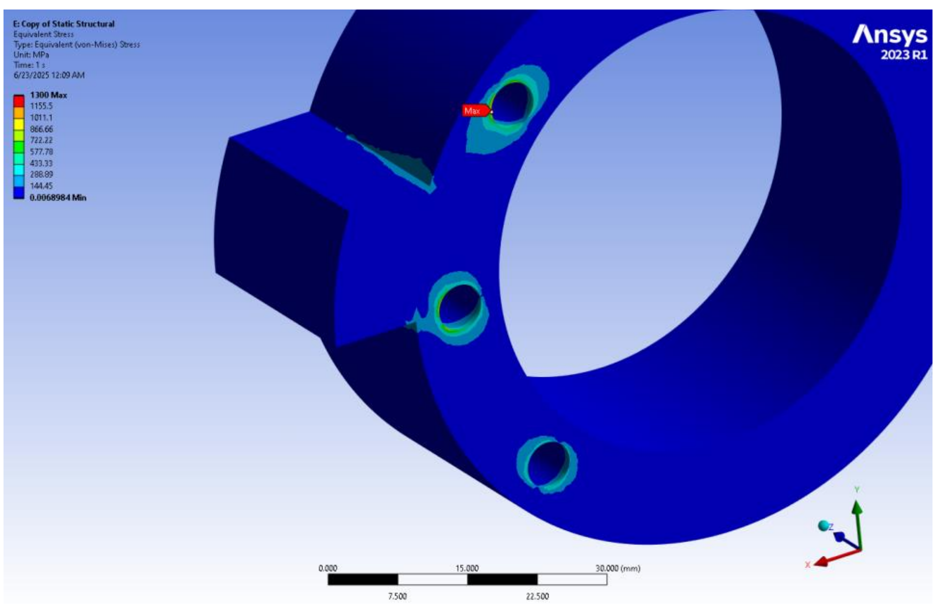

Figure A 51 - ANSYS – 14kN CAPSTAN HOLE CLOSEUP - von-Mises stress

Figure A52 illustrates the same region at a higher load of 14 kN. A noticeable increase in von Mises stress is observed around the hole perimeter, confirming it as a critical area for stress concentration and potential plastic deformation under full loading.

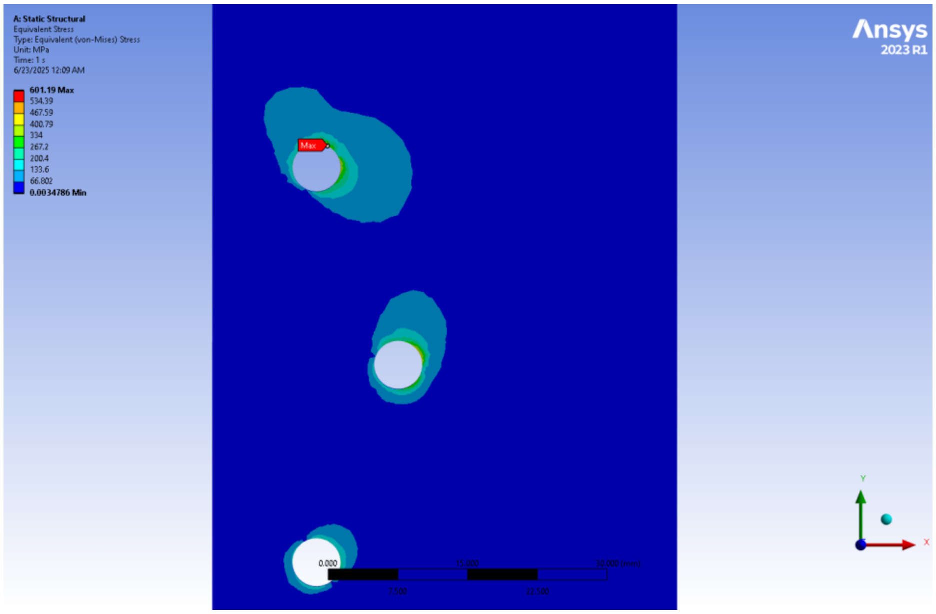

Figure A 52 - ANSYS - 7.1kN Body Hole Close Up - von-Mises stress

Figure A53 presents the factor of safety (FoS) distribution across the Capstan grip under a 13 kN load. Most of the structure maintains a safety factor above 2.0, indicating sufficient design margins for this load level, with the exception of small localized stress risers.

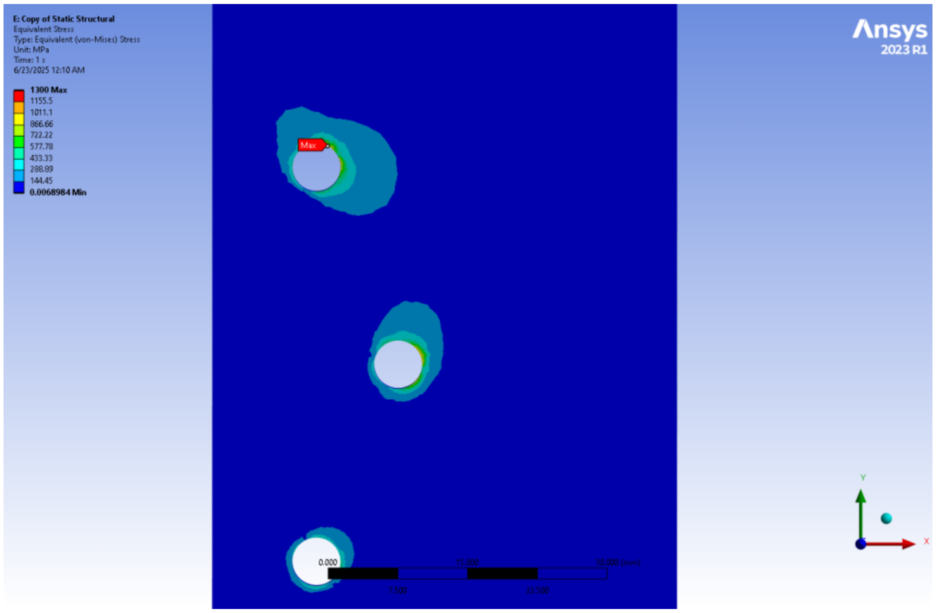

Figure A 53 - ANSYS - 14Kn Body Hole Close Up - von-Mises stress

Figure A54 focuses on the bolt region's safety factor under the same 13 kN loading. The area directly adjacent to the threads and bearing surfaces shows reduced FoS values, approaching critical limits, highlighting the importance of bolt sizing and preload.

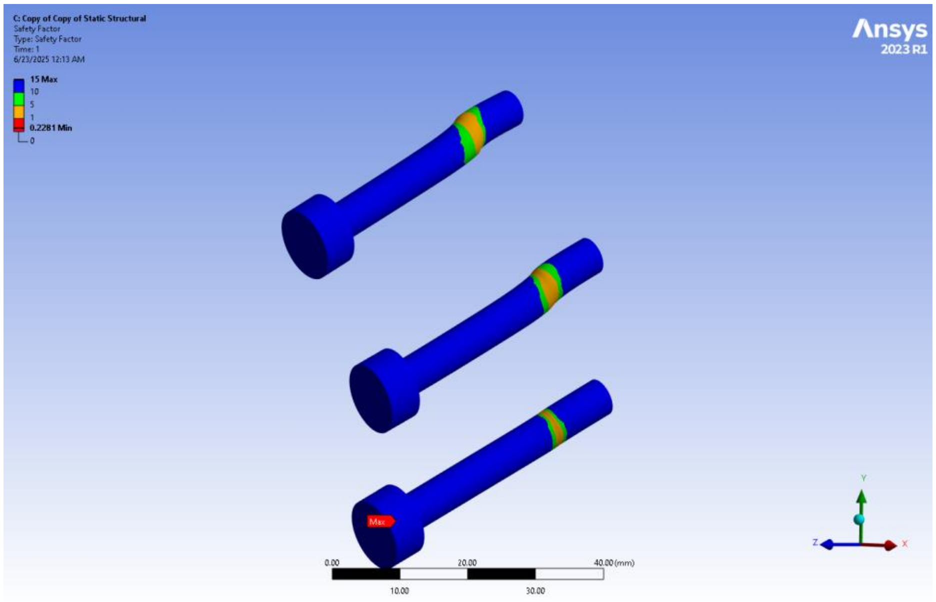

Figure A 54 - ANSYS - FoS of Bolt 13kN

Figure A55 shows the safety factor distribution at 27 kN, which represents the doubled load condition (FoS = 1). The bolts and surrounding metal display FoS values approaching 1.0, confirming that this is the design's maximum allowable safe load before yielding.

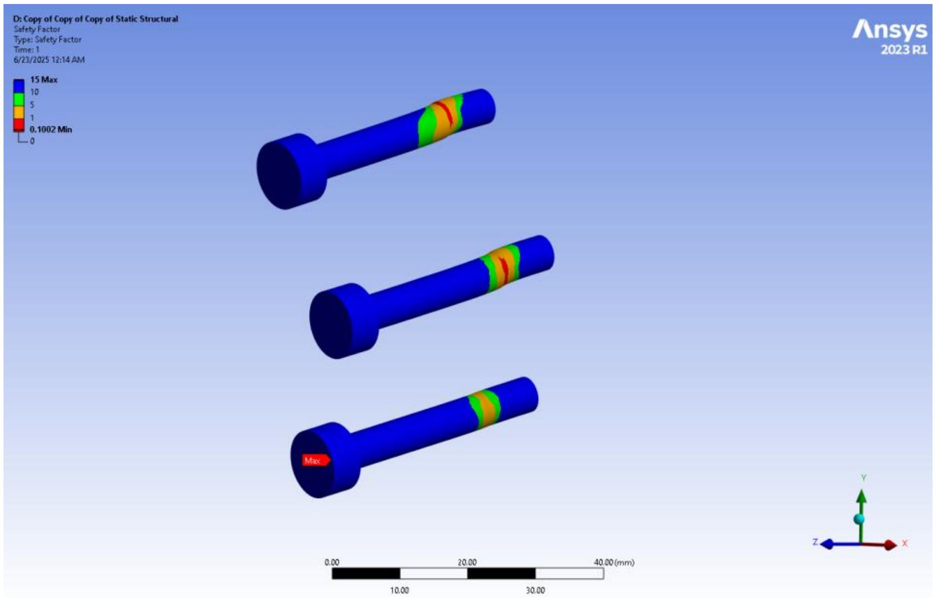

Figure A 55 - ANSYS - FoS of Bolt - 27kN

Figure A56 illustrates the factor of safety across the simplified Capstan model under a 13 kN load. The simplification retains the critical features of the geometry while reducing computation time. The stress distribution remains consistent with the full model, confirming accuracy.

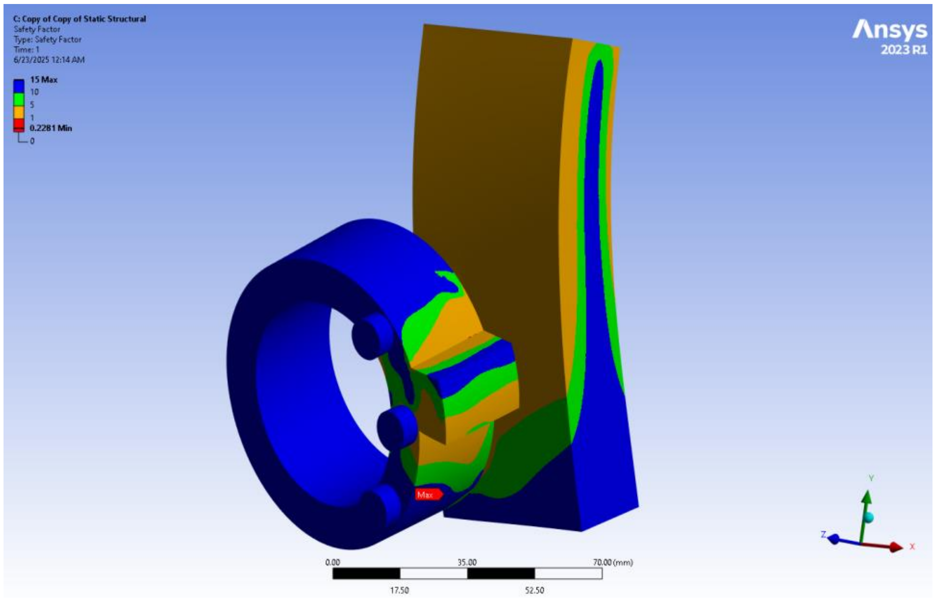

Figure A 56 - ANSYS - FOS of Simplified Model at 13kN

Figure A57 shows the same simplified model under a 27 kN load condition, equivalent to the yield threshold (FoS = 1). The most vulnerable zones, particularly near bolt holes and capstan surfaces, approach the material's yield strength, validating the safety limit previously established.

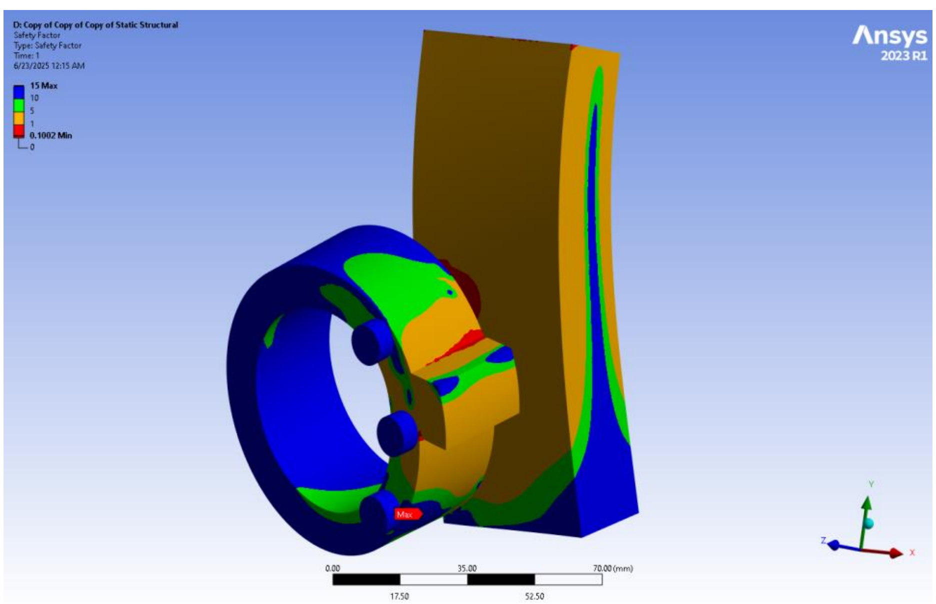

Figure A 57 - ANSYS - FOS of Simplified Model at 27kN

Figure A58 compares the von Mises stress distribution between the full assembly and its simplified counterpart under 13 kN. The consistency of peak stress locations between both models confirms that the simplified approach is valid for evaluating structural safety.

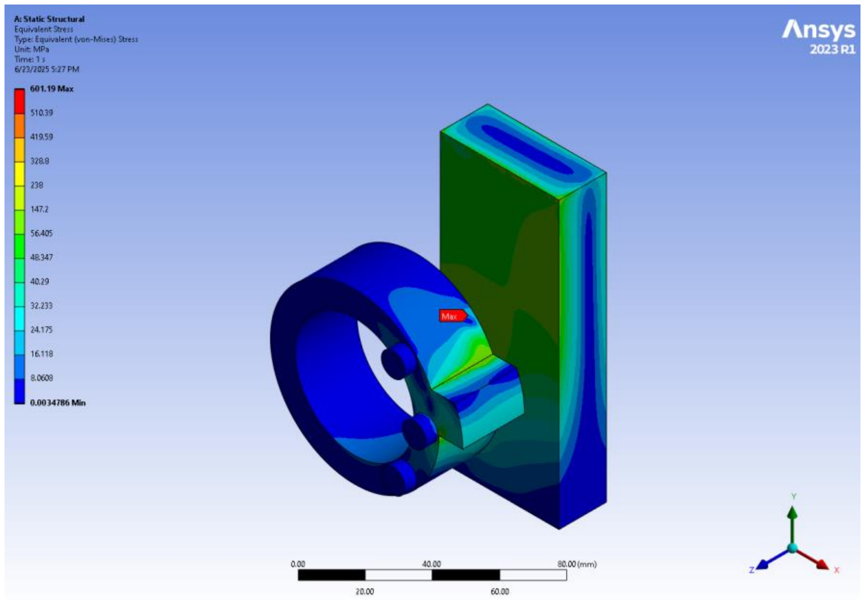

Figure A 58 – 7152N – von-Mises of Model

Figure A59 visualizes total deformation across the full Capstan assembly under 27 kN. Maximum deflections occur at the clamp arms and rope interface, but remain within elastic limits, ensuring grip functionality without permanent deformation.

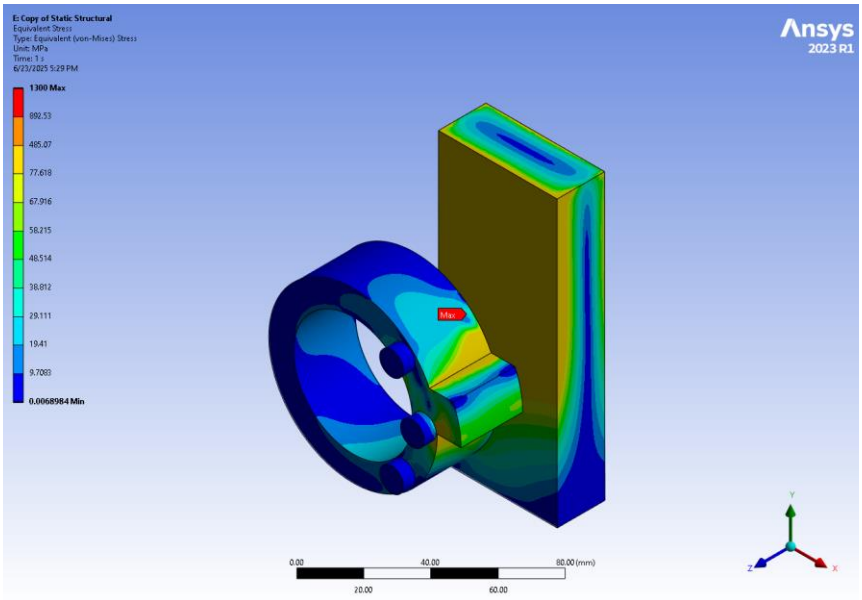

Figure A 59 - 1403N - von-Mises of Model

Figure A60 displays displacement results for the simplified model under the same loading. Deformation patterns mirror those of the full model, further validating the use of simplification in the stress analysis phase.

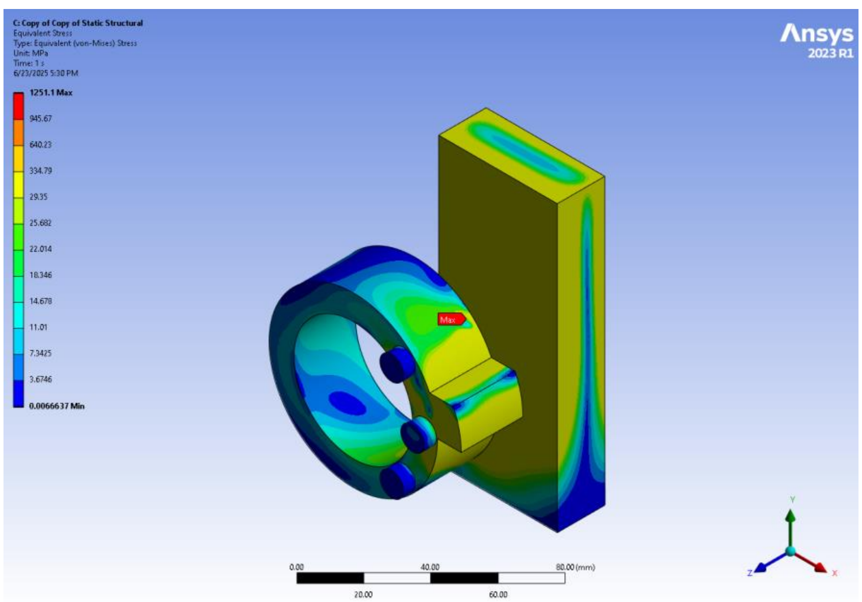

Figure A 60 - 13812N - von-Mises of Model

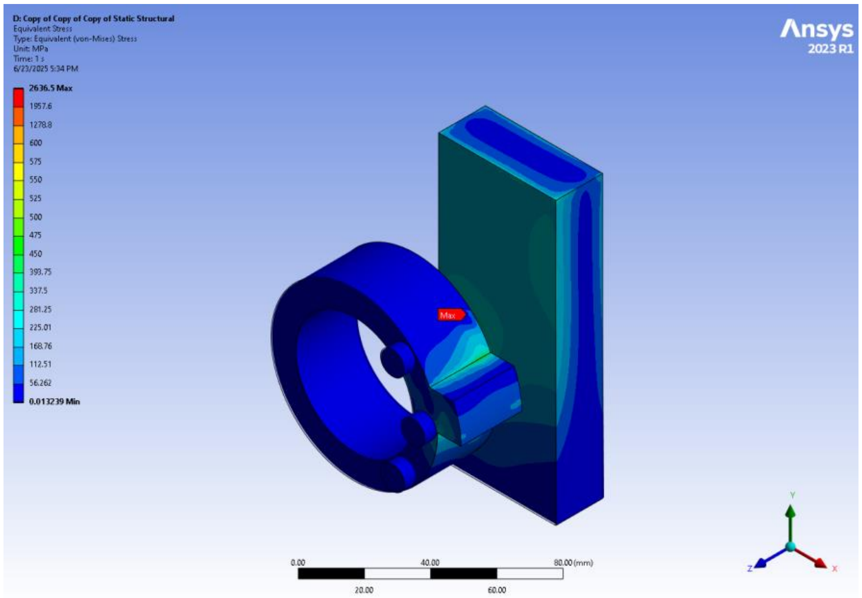

Figure A 61 - 27625N - von-Mises of Model

CURRICULUM VITAE

Barış TAPAN

Education

B.Sc. in Mechanical Engineering

Marmara University, Istanbul, Turkey

2019-Present

High School Diploma

Nazmi Arıkan Fen Bilimleri Temel Lisesi, Istanbul Turkey

2015-2019

Internships & Work Experience

Marketing Intern

Motul – Istanbul, Turkey

May 2024 – October 2024

- Supported the management of social media and digital marketing activities.
- Contributed to brand awareness efforts through event organization and promotional campaigns.
- Assisted in developing and implementing marketing strategies.
- Coordinated communications with regional representatives, partners, and third parties to support operational workflows.

Engineering Intern

Sınai İmalat Otomotiv San. ve Tic. A.Ş. – Istanbul, Turkey

August 2023 – September 2023

- Observed production line operations and supported quality control processes.
- Assisted in maintenance and operational procedures of production machinery.
- Worked on technical drawings and basic engineering calculations.
- Provided efficiency analysis and improvement suggestions.

Skills & Competencies

Languages:

- Turkish. Native
- English: C1 (Advanced)

Software & Tools:

- AutoCAD
- SolidWorks

Certificates

- Planning and Management of Research

Interests

- Active defensive player in the **Turkish National Lacrosse Team**
- Mapping & level design using **Unreal Engine**

Mohamed Tharwat ELNAGAR

Profile

Final-year Mechanical Engineering student at Marmara University with a strong interest in material science and composite structures. Known for punctuality, eagerness to learn, and excellent teamwork and communication abilities. Actively seeking opportunities to apply technical knowledge in dynamic, innovative-driven engineering environments, with the goal of contributing to cutting-edge solutions in the field.

Education

B.Sc. in Mechanical Engineering

Marmara University, Istanbul, Turkey

2019-Present

Internships & Work Experience

Intern – Machinery & Equipment Maintenance + Rotational Internship

Chelsea Ground Engineering — Khobar, Saudi Arabia

Jul 2024 (30-day internship)

- Completed a general internship across multiple departments, gaining exposure to operations, safety, and technical processes.
- Focused on machinery and equipment maintenance tasks, learning about preventive systems and engineering protocols.
- Assisted technicians with diagnostics, repairs, and workshop documentation.
- Developed an understanding of cross-department collaboration in a field environment.

Skills & Competencies

Technical Skills:

- SolidWorks
- AutoCAD
- MATLAB
- Microsoft Office (Excel, Word, PowerPoint)
- Basic knowledge of CNC machinery and workshop tools
- Understanding of maintenance systems and equipment diagnostics

Soft Skills:

- Team collaboration and communication

- Time management and punctuality
- Problem-solving mindset
- Adaptability and eagerness to learn
- Professional work ethic

Languages:

- Arabic: Native
- English: Advanced
- Turkish: Beginner

EXTRACURRICULAR ACTIVITIES

- Football player for the Faculty of Engineering Team, Marmara University — participated in university-level tournaments, demonstrating teamwork, discipline, and commitment.